

**This dissertation has been
microfilmed exactly as received**

66-14,197

**BOGGS, John Vincent, 1940-
GAMMA-RAY SPECTRA OF FISSION PRODUCTS
FROM U²³⁵ AS A FUNCTION OF TIME AFTER
FISSION.**

**The University of Oklahoma, Ph.D., 1966
Physics, nuclear**

University Microfilms, Inc., Ann Arbor, Michigan

THE UNIVERSITY OF OKLAHOMA

GRADUATE COLLEGE

GAMMA-RAY SPECTRA OF FISSION PRODUCTS FROM U^{235}
AS A FUNCTION OF TIME AFTER FISSION

A DISSERTATION

SUBMITTED TO THE GRADUATE FACULTY

in partial fulfillment of the requirements for the

degree of

DOCTOR OF PHILOSOPHY

BY

JOHN V. BOGGS
INCENT

Norman, Oklahoma

1966

GAMMA-RAY SPECTRA OF FISSION PRODUCTS FROM U^{235}
AS A FUNCTION OF TIME AFTER FISSION

APPROVED BY

Albert E. Wilson
Edwin H. Kehr
J. H. Bugnelli
Frank Caspelli
Raymond D. Daniels
Jack Reynolds

DISSERTATION COMMITTEE

ACKNOWLEDGEMENT

The author wishes to express his sincere gratitude to the many individuals from whom assistance and encouragement have been obtained in the preparation of this dissertation. In particular, appreciation is extended to Dr. A. E. Wilson for the advice and stimulation given during the study.

The assistance and interest of the entire staff of Group P-2 of the Los Alamos Scientific Laboratory is sincerely appreciated. Most sincere thanks are due to Dr. E. T. Journey and Dr. H. T. Motz for their advice and direction of the study.

Thanks are also extended to the Associated Rocky Mountain Universities and to the Atomic Energy Commission for financial assistance during the program.

TABLE OF CONTENTS

| | page |
|--|------|
| LIST OF TABLES | v |
| LIST OF ILLUSTRATIONS | vi |
| CHAPTER | |
| I. INTRODUCTION | 1 |
| II. REVIEW OF PREVIOUS WORK | 4 |
| III. PREDICTION OF RESULTS | 8 |
| IV. EXPERIMENTAL PROCEDURE AND EQUIPMENT | 26 |
| V. DATA REDUCTION AND EXPERIMENTAL RESULTS | 43 |
| VI. DISCUSSION OF RESULTS | 69 |
| LIST OF REFERENCES | 75 |
| APPENDICES | |
| A. DERIVATION OF VARIATIONS OF THE BATEMAN EQUATIONS | 79 |
| B. COMPUTER PROGRAM FOR THE PREDICTION OF FISSION- PRODUCT GAMMA-RAY SPECTRA | 87 |

LIST OF TABLES

| | page |
|---|------|
| 1. COUNTING INTERVALS AND MEAN TIMES FOR THE ANALYZER SUBGROUPS..... | 48 |
| 2. IRRADIATION TIMES AND NUMBER OF SUBGROUPS FOR THE ENERGY INCREMENTS | 48 |
| 3. GAMMA ACTIVITY FOR EACH ANALYZER SUBGROUP, SHORT TIMES | 53 |
| 4. GAMMA ACTIVITY FOR EACH ANALYZER SUBGROUP, LONG TIMES | 59 |
| 5. IDENTIFIED FISSION PRODUCTS | 72 |

LIST OF ILLUSTRATIONS

| Figure | | page |
|--------|--|------|
| 1. | Cs ¹³⁷ SPECTRUM AND COMPUTED SPECTRUM | 14 |
| 2. | PREDICTED SPECTRUM AT 52 MINUTES AFTER FISSION | 25 |
| 3. | BLOCK DIAGRAM OF DATA ACCUMULATION EQUIPMENT | 31 |
| 4. | PLAN VIEW OF EXPERIMENT | 32 |
| 5. | SAMPLE OUTPUT OF FITTING PROGRAM | 46 |
| 6. | EFFICIENCY CURVE FOR DETECTOR | 50 |
| 7. | FISSION PRODUCT GAMMA RAY SPECTRA, 0.4-2.9 SECONDS AFTER FISSION | 65 |
| 8. | FISSION PRODUCT GAMMA RAY SPECTRA, 2.9-42 SECONDS AFTER FISSION | 66 |
| 9. | FISSION PRODUCT GAMMA RAY SPECTRA, 0.7-9.7 MINUTES AFTER FISSION | 67 |
| 10. | FISSION PRODUCT GAMMA RAY SPECTRA, 9.7-152.7 MINUTES AFTER FISSION | 68 |
| 11. | COMPARISON OF PREDICTED SPECTRUM WITH EXPERIMENTAL SPECTRUM AT 14.7 MINUTES AFTER FISSION | 71 |

GAMMA-RAY SPECTRA OF FISSION PRODUCTS FROM U^{235}

AS A FUNCTION OF TIME AFTER FISSION

CHAPTER I

INTRODUCTION

A detailed study of the slow-neutron fission of uranium-235 has shown that the compound nucleus splits up in more than 40 different ways, yielding over 80 primary fission products (fission fragments). The range of mass numbers of the fragments is from 72 to 166. The masses of nearly all the fission products fall into two broad groups, a "light" group, with mass numbers from 80 to 110, and a "heavy" group, with mass numbers from 125 to 155. The product masses which lie between and outside these ranges represent not more than a few per cent of the fissions. The most probable type of fission, comprising nearly 6.4 per cent of the total, gives products with mass numbers 95 and 139. It is apparent that the slow-neutron fission of uranium-235 is unsymmetrical in the great majority of cases.

The fragments generally do not represent nuclei in their normal states, since both fragments can carry considerable excitation energy. The light fragment's average excitation energy is approximately 11 MeV; that of the heavy one approximately 9 MeV. The proton-to-neutron ratio of the fragments is less than that of the stable nuclei, the fragments being neutron rich. The excited

fragments behave, on the whole, as do other nuclei with high excitation energy: they approach more stable configurations by the emission of particles and gamma rays. The most probable adjustment is beta decay which results in an approach to the more stable ratio of protons to neutrons. If a heavy particle is emitted, as occasionally occurs, it would be a neutron.

Even after the emission of the prompt neutrons, both fragments remain about three atomic numbers removed from the condition of maximum stability, and both have to undergo about three successive beta decays before a stable nucleus results. The group of nuclei formed by the successive beta decays of a fission fragment is called a "decay chain". Although the average length of these chains is three decays, the individual lengths vary from as little as one decay to as many as six decays in rare instances.

With each beta emission there are usually one or more associated gamma rays. Because of the penetrating nature of these gamma rays it becomes necessary to shield the fission products in the fuel elements of nuclear reactors. In order to prepare an adequate shield the designer must have certain information on the fission product gamma radiation. Ideally he must know the energy, the half-life, and the activity or intensity of each fission product gamma ray as a function of time, and also he must know whether or not a particular fission product nuclei has a parent. This information is well known for fission products of long half-lives and for times after fission exceeding a few hours, but little accurate information is known for short times after fission.

There are significant but not insurmountable problems associated with observing a gamma ray spectrum at short times after fission. The target sample must be removed from the neutron flux as rapidly as possible and positioned in front of the detector system, which must then be started as soon as possible. A large and versatile data handling system must be utilized to allow several time-dependent gamma-ray spectra to be studied. The number of fission product gamma rays (nearly 1000 known) necessitates a detection system which has excellent resolution in order that a large number of these gamma rays can be individually evident in the spectra. In order to obtain a true representation of the gamma spectra at short times the build-up of long-lived isotopes must be minimized by using short irradiation times. In order to study the gamma spectra of short-lived fission products, short counting times must be used. The combination of short counting times and short irradiation times will give poor counting statistics for samples of relatively low mass.

The mass of the sample must be low to avoid the self-shielding of low-energy gamma rays. To improve the counting statistics a cycling procedure in which the same sample is reirradiated and counted could be used, but this again introduces the problem of long-lived isotope build-up. Alternatively, a number of samples could be used with each counting cycle seeing a "fresh" sample. Delayed neutrons may be significant shortly after fission, not only causing possible detector damage but also producing undesirable background gamma rays following neutron capture in the surrounding equipment. Because of the short times and the many cycles required, an automatic program for switching and timing is required to insure reproducibility.

CHAPTER II

REVIEW OF PREVIOUS WORK

Almost all the observations of fission product gamma ray spectra have been done using a NaI (Tl) scintillation crystal as the detector. These detectors can be quite large and have good detection efficiency, but relatively poor energy resolution. As a result, the observed fission product gamma ray spectrum shortly after fission is a continuum with few distinguishable peaks. Many of the investigators have resorted to breaking this continuum down into several energy groups, or "bins" as some authors prefer to call the groups, and observing the gamma emission with single-channel analyzers. They then connect the separately measured group activities into a continuous "spectrum".

Zigman and Mackin [1] have reported gamma activity and spectra of fission products after thermal neutron fission of U^{235} . Their continuum spectrum consisted of 12 energy groups ranging in energy from 20 keV at the bottom of the lowest energy group to 5500 keV as the upper limit for the highest energy group. They reported activities for these groups at times after fission ranging from 1.0 second to 1.74×10^4 seconds. Two sources of data were used in the above report. One source consisted of measurements following U^{235} fission by thermal neutrons made at the United States Naval Radiological Defense Laboratory

(USNRDL). The other and primary source of data was the Knabe and Putnam [2] summary of Oak Ridge measurements following fission by thermal neutrons [3] [4] [5] [6] [7].

Gamma activity and energy spectra of fission product following fission by a 50 msec burst of fission spectrum neutrons from the Godiva II Critical Assembly have been measured by Engle and Fisher [8]. They, too, used the group method and their spectra have the resultant stair-step form. Their data show that the gamma decay rate following U^{235} fission by fission spectrum neutrons from Godiva II agrees closely with the gamma decay rate following U^{235} fission by thermal neutrons.

Petrov [9] has investigated the gamma activity of fission products of U^{235} and Pu^{239} from 0.6 second to 11 hours after targets were subjected to "pulsed irradiation" in the thermal neutron flux of the heavy-water nuclear reactor at the Academy of Sciences, USSR. The short duration irradiation of the targets (1 second) was accomplished by a pneumatic transfer system. Petrov reported that within the limits of experimental error (10%) the gamma activities of U^{235} and Pu^{239} fission products have the same decay kinetics, the same mean energies of the gamma quanta, and the same total gamma ray energy-yield per fission. His work was done with the use of geiger counters and ionization chambers. With the high resolving capability of present-day detection equipment it would be relatively easy to compare the fission product gamma spectra of U^{235} and Pu^{239} .

The results of Zigman and Mackin, Engle and Fisher, and Petrov are in reasonable agreement. From 0.1 second to 40 seconds after fission the measurements are within approximately 10% of each other. For times

greater than about 40 seconds the measurements by Petrov are increasingly larger than the measurements reported by Zigman and Mackin.

Miller [10] has calculated the gamma activity of fission products after slow neutron fission of U^{235} for times greater than about 46 minutes after fission. The gamma activity was calculated by multiplying the values of energy (MeV) per disintegration and photons per disintegration from Miller [11] by the values of disintegrations per second at the given times after fission from Bolles and Ballou [12]. In the region in which times overlap the calculations by Miller are nearly identical with the measurements by Zigman and Mackin. Miller also calculated the average photon energy of U^{235} fission products for times greater than one hour after fission.

There are two facts that are evident from the above analysis: (1) gamma activity and spectra following fission of U^{235} by thermal neutrons coincide with that of fission of U^{235} by fission spectrum neutrons, and (2) gamma activities of U^{235} fission products and Pu^{239} fission products are identical within limits of experimental error.

John Moteff [13] made a theoretical study of fission product gamma ray spectra as a function of time after shutdown of a reactor and also as a function of operating or irradiation time. He divided the energy spectrum into seven energy groups and calculated the activities of each group as a function of time after shutdown and of various operating times.

F. H. Clark [14] extended Moteff's work to include short times after shutdown. His work was a little more detailed due to the accumulation of additional experimental data. Clark also used seven energy

groups but went further by calculating the activity (MeV/watt-second) of every prominent isotope in each group as a function of time after shutdown and of reactor operating time.

Other work in the field has been done by Perkins and King [7] who reported that the gamma spectrum shape depends fairly strongly on decay time but only weakly on reactor operating time. McBean [15] studied the energy of fission fragments as a function of time. He indicates that the highest energy release (energy/fission-second) occurs between 10 and 100 seconds after fission.

At the time of this writing there is no published evidence that anyone has observed and analyzed fission product gamma ray spectra with the aid of high resolution solid state detectors. Although Armantrout and Camp [16], and John [17], working with solid state detectors (germanium lithium-drift), have observed a fission product gamma ray spectrum, it is exhibited in their report mainly as a demonstration and no analysis of the spectrum, other than the identification of thirteen known isotopes using only the more prominent peaks, is given.

CHAPTER III

PREDICTION OF RESULTS

In order to predict the pulse height spectrum for a germanium detector for a mixture of fission products, a computer program was developed to simulate fission product decay and detector response.

There are a number of reasons for trying to predict the shape of a fission product gamma ray spectrum. Foremost, of course, is the fact that the "spectra" can be used as aids in identifying prominent peaks in the experimentally observed spectra. A considerable amount of analysis time can be saved by looking only at those peaks which were not predicted and are, thus, "unknown". The buildup and decay of certain known isotopes can be observed, thus demonstrating the effect of short-lived precursors. A series of time-dependent spectra can actually be used as a "dry run" simulating the results of the actual data-taking. The accuracy of these spectra depends on the accuracy of the known data. By comparing the actual spectra with the predicted "spectra" a check can be made of the accuracy of the literature values of relative chain yields and perhaps better values will result.

In order to obtain a good predicted spectrum (in the sense of the best information available) every known radioactive fission product must be used. Each radioactive fission product must be

cataloged with the following information: isotopic fission yield, half-life, number and energy of gamma rays, branching ratio for each gamma ray (corrected for possible internal conversion), the possible existence of an isomeric state and if one does exist, its half-life, number and energy of gamma rays, fission yield, and manner of decay. In most cases, all of the above information with the exception of fission yields was obtained from the latest values presented in the Nuclear Data Sheets [18] and Crocker and Conners [19]. Available fission yield data were taken from Katcoff [20] and England [21]. Of course not all the above information is available for all the fission products. In cases where such data are lacking the values were estimated. The estimation of missing fission yields can be considered fairly good since, for almost every decay chain, the total chain yield is known. According to Pappas [22], there exists a distribution about a most probable atomic number of the total chain yield. Using this fact and his table of most probable atomic numbers, a good estimate of isotopic yield can be obtained.

There exist about 1000 known fission product gamma rays. Many of these gamma rays will not be observed in a fission product spectrum due to low branching ratios, low chain or isotopic yields, long half-lives, or combinations of these. Some discretion, therefore, must be used to avoid performing time-consuming calculations on those gamma rays which will not contribute appreciably to the predicted spectrum. As a general rule, those gamma rays with a relative intensity or branching ratio less than one per cent of the most prominent gamma's intensity or branching ratio may be discarded. This culling reduces the total to 800 gamma rays. These gamma rays are distributed over 81 different mass

chains and about 200 fission products.

In order to compute the spectra, each fission product activity as a function of time must be calculated. This may be done with the well-known Bateman equations which give the isotopic concentration of any isotope in a constant mass decay chain at any time. There are three variations of these equations specifically dealing with fission products in a single constant mass decay chain. One is the continuous production variation, i. e., the concentration of fission products while the fissionable isotope is being irradiated:

$$N_{i,1} = \lambda_1 \lambda_2 \lambda_3 \cdots \lambda_{i-1} P_1 \sum_{j=1}^i \frac{1 - e^{-\lambda_j T}}{\lambda_j \prod_{k \neq j} (\lambda_k - \lambda_j)} \quad (1)$$

$$N_i = N_{i,1} + N_{i,2} + \cdots + N_{i,i} \quad (2)$$

where $N_{i,m}$ = number of atoms of i-th isotope in chain due to the decay of the m-th isotope at time T after beginning of production.

λ_i = decay constant of i-th isotope.

P_m = constant rate of production of m-th isotope

$$= \Sigma_f \varphi y_m$$

where Σ_f = macroscopic fission cross section of fissionable isotope.

φ = neutron flux

y_m = fission yield of m-th isotope.

N_i = total number of atoms of i-th isotope present at time
T due to decay of all precursors and production of i-th
isotope ($N_{i,i}$).

T = time since constant production began.

Another variation is the batch decay after shutdown:

$$N_{i,1} = \lambda_1 \lambda_2 \lambda_3 \cdots \lambda_{i-1} N_1^0 \sum_{j=1}^i \frac{e^{-\lambda_j t}}{\prod_{k \neq j} (\lambda_k - \lambda_j)} \quad (3)$$

$$N_i = N_{i,1} + N_{i,2} + \cdots + N_{i,i} \quad (2)$$

where N_m^0 = number of atoms of m-th isotope present at time
of shutdown.

t = time after shutdown.

The last variation is a combination of the two previous conditions,
namely, continuous production and shutdown:

$$N_{i,1}(T,t) = \lambda_1 \lambda_2 \lambda_3 \cdots \lambda_{i-1} P_1 \sum_{j=1}^i \frac{(1-e^{-\lambda_j T}) e^{-\lambda_j t}}{\lambda_j \prod_{k \neq j} (\lambda_k - \lambda_j)} \quad (4)$$

$$N_i(T,t) = N_{i,1} + N_{i,2} + \cdots + N_{i,i} \quad (2)$$

where $N_i(T,t)$ is the number of atoms of the i-th isotope present after
a reactor operating time T and a shutdown time t. These equations are
derived in Appendix A. The appropriate set of equations to use in the

prediction of spectra would be equations (4) and (2), the continuous production and shutdown set. These spectra, however, are designed to be matched with the experimental results and for short irradiation times ($\lambda T \ll 1$) the production term,

$$(1 - e^{-\lambda_j T})/\lambda_j, \approx T$$

for all isotopes and the general shape of the spectrum will remain unchanged. If this approximation is made, equation (4) reduces to the batch decay set, equation (3).

Because of the complexity of the Bateman equations and the enormous number of values of basic data, the problem of predicting a spectrum was accomplished by means of a computer code. The computer must necessarily have a large memory and should possess the capability for plotting the results. A listing of the program along with a flow chart appears in Appendix B.

The calculations proceed by chains through all mass chains with the initial value of each isotope, N_i^0 , being set equal to the fission yield, y_i , of that particular isotope. This is not really correct since

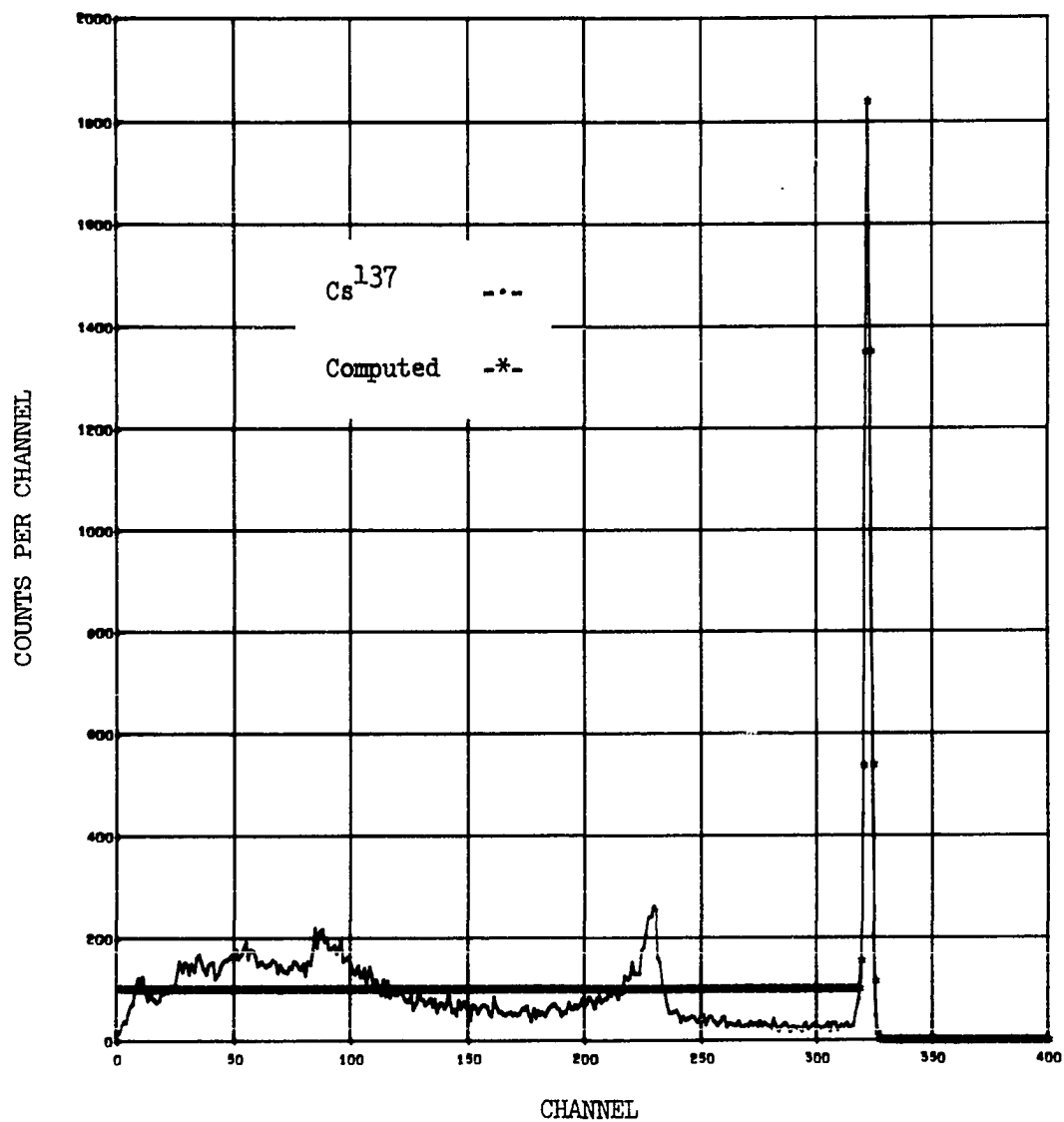
$$N_i^0 = \Sigma_f \phi y_i. \quad (5)$$

However, the value, $\Sigma_f \phi$, will be the same for all fission products and will, thus, not affect the shape of the spectrum. The activity values calculated will not be correct absolute values unless they are multiplied by the value, $\Sigma_f \phi$, for the particular target mass and flux

of interest.

Once the concentration of a particular isotope at a certain time has been determined by the Bateman equations, the activity of that isotope is calculated by multiplying by its decay constant. This isotopic activity is then distributed among the isotope's gamma rays. The gamma activity is obtained by multiplying the isotopic activity by the gamma ray's branching ratio. In order to obtain a more nearly true spectrum, this activity is multiplied by the detector efficiency at the particular gamma ray energy since the solid state detector efficiency is strongly dependent on energy. This is considered in more detail later.

We now have the interaction rate in the detector for a particular gamma ray. In order to simulate a detector, the gamma ray intensity is distributed in such a way as to most closely resemble the actual detector response. By observing the spectra of selected radioisotopes with single gamma rays the simplest detector response was determined to be a gaussian peak with a constant tail extending all the way to zero energy (Fig. 1). The amplitude of this tail for the particular detector used was estimated to be one per cent of the area of the gaussian peak. This value may vary from detector to detector. The detection system that was used (Chapter IV) is of the anti-coincidence type [23] where the Compton edge is effectively suppressed. The observed tailing is believed to be partly due to an "edge" effect, where the interaction which converts gamma ray energy to electron energy occurs in the proximity of a boundary, or edge, of the detector. The electron loses only part of its energy before escaping, giving the effect of observing a lower



Cs^{137} SPECTRUM AND COMPUTED SPECTRUM

FIGURE 1

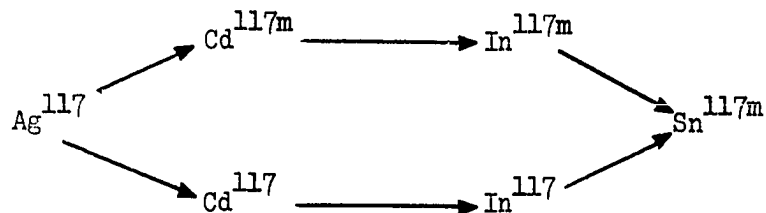
energy gamma ray. It can be observed that there is no Compton edge in the simulated distribution.

For gamma rays above 2.0 MeV the detection system can be used in the double-escape coincidence mode in which case the Compton edge is completely suppressed. Although no data were taken in the double-escape mode, for purposes of calculation over the complete simulated spectrum this mode will be considered. The resolution (full width half maximum) of the gaussian peak must be known before the distribution can be calculated. It is a function of energy and can be calculated for each gamma ray. This function is determined by detector parameters and is discussed in more detail later. Each gamma ray activity is represented by a gaussian distribution, the tail is added on, and the result is then stored in a one-dimensional matrix according to the energy of the gamma ray. The activities assigned to locations in this matrix are added to values already present in those particular locations.

The calculation proceeds until all of the gamma rays of the isotope have been assigned to the proper locations in the matrix. The program then flows on to the next isotope and its gamma rays, and so on, until every gamma ray of each isotope in the chain has been assigned an activity distribution in the matrix. The same procedure applies to all decay chains until all the gamma rays have been assigned locations in the matrix. The matrix is then plotted and becomes the predicted spectrum.

The Bateman equations assume beta decay for the transition from one isotope to the next. A complication thus arises when an isomeric

state exists in one of the isotopes. This problem is easily solved when the transition percentages from the parent to each of the isomers is known. In this case the lower energy isomer occupies its normal position in the chain, but its isotopic activity is multiplied by its transition fractions before the gamma activities are calculated and stored. Then this isotope is replaced by its isomer before proceeding on to the next member of the decay chain. This isomeric activity is calculated and multiplied by its transition fraction followed by the calculation of its gamma activities. The calculations then proceed in the normal manner through the remainder of the decay chain making sure that the original isomer is replaced into its normal position. This procedure is used when the higher energy isomer decays only by isomeric transition, or when both isomers decay to a stable or long lived daughter. In the cases where both isomers undergo beta decay and/or when the transition percentages from the parent nuclide are unknown, a second dummy chain must be used. This accounts for the fact that there are 97 decay chains for 81 masses. The precursors in the dummy chain must necessarily have a fission yield of zero to keep from calculating the same gamma activities twice. The daughters in the dummy chain must have a yield of zero so that their gamma activities will be calculated only by contribution of the new isomers and not as a result of direct fission yield. This can be illustrated by an example. Consider mass number 117 and its associated decay chain:



The top route is chain number 49 and the bottom is number 50. In chain 50 the $\text{Sn}^{117\text{m}}$ nuclide has a fission yield of zero as does the Ag nuclide since these yields are accounted for in chain number 49. The transition percentages to the Cd isomers are unknown and are thus assumed to be equal. This introduces errors in the calculation of the Cd gamma activities, but since the isomers usually have low fission yields these errors are insignificant.

The spectra are intended to be representative of detector response so some detector-dependent parameters are needed. Most notable are those of efficiency for correct gamma activities and resolution for a true peak shape. The detector's efficiency depends strongly on the energy of the incident gamma ray. At fairly low energies, less than 200 keV, the peak efficiency is relatively high since the majority of interactions between gamma rays and Ge atoms are photoelectric. In this case the entire energy of the photon is given over to an electron which easily dissipates all its energy within the detector. As the energy of the photon increases, however, the photoelectric absorption cross section for germanium drops off very rapidly and the predominant interaction becomes Compton scattering in which only a part of the energy of the gamma is converted to electron energy within the detector, except for those events in which the

scattered Compton gamma ray is also converted. The efficiency of the detector operating in the anti-coincidence mode is very nearly proportional to the photoelectric absorption cross section for germanium. The efficiency relationship was determined in the normal manner by using known activity radioisotopes. The shape of this curve, as expected, was similar to the photoelectric cross section curve. The response curve can be closely approximated as the sum of two exponential functions with negative exponents.

$$I(E) = Ae^{-\alpha_1 E} + Be^{-\alpha_2 E}, \quad E \leq 2800 \text{ keV} \quad (6)$$

It is assumed that all solid state detector efficiency curves will have this same general shape. This function was therefore included in the program with four variable input parameters.

When the energy of a gamma ray is greater than twice the rest energy of an electron, pair production can take place inside the detector. The kinetic energy of the positron-electron pair is equal to the energy of the gamma ray minus the 1022 keV required to produce the pair, and this kinetic energy is dissipated in the detector. The energy resulting from the annihilation of the positron appears as two gamma rays of 511 keV each which can leave the detector without interaction. Although the pair production cross section in germanium increases rapidly with energy, edge effects again play an important part in determining the shape of the efficiency curve. At very high energies (>5 MeV) energy loss by bremsstrahlung also will be important. For these reasons, instead of following the shape of the pair production

cross section curve, the efficiency of the detector operated in the double escape coincidence mode tends to be constant with energy up to about 4 MeV in gamma ray energy at which point the efficiency begins to decrease. The function determined for this shape was a constant minus an exponential term:

$$I(E) = C - D \cdot e^{\delta E}, \quad 2800\text{keV} < E < 6000 \text{ keV}. \quad (7)$$

Unlike the efficiency function used for the anti-coincidence mode of operation, this function is dependent on detector volume. In the case of a large detector it is expected that the efficiency will actually increase with energy before the decrease.

With these two functions (seven input parameters) placed in the program the efficiency of the detector for any fission product gamma ray can be determined and a representative spectrum can be calculated.

The other important detector parameter is resolution, the ability to distinguish or resolve two or more gamma rays with energies close to each other. A detector with poor resolving ability might depict two gamma rays with nearly the same energies as one broad peak while a detector with better resolution would depict these two gamma rays as two distinct peaks. Two inherent factors contribute to line broadening. One of these is the small component of noise arising in the preamplifier which instantaneously adds to or subtracts from the amplitude of a given pulse. The other contribution to line broadening is the statistical variations in the number of electron-hole pairs created by a gamma ray

of a given energy and consequently collected. The energy required to create a hole-electron pair in Ge is ~ 2.9 eV; thus, for example, a 2.9 MeV gamma ray converted to a single high-energy electron in germanium will produce 10^6 pairs, and the standard deviation in this sample will be the order of 10^3 pairs, or $\sim 0.1\%$. The line width resulting from a combination of the noise component and the component arising from the statistical variation in the number of electron-hole pairs can be approximated by:

$$\sigma^2 = d^2 + kE_\gamma \quad (8)$$

σ = line width (FWHM)

d = noise component (keV)

k = proportionality constant

Equation (8) applies only when the detector system is operated in the anti-coincidence mode. In the coincidence mode in which only the energy dissipated by the hole-electron pairs in coincidence with two annihilation gammas is counted, the statistical component of broadening is not proportional to the energy of the incident gamma ray but proportional only to the number of hole-electron pairs created. This number is proportional to the square root of the gamma energy minus twice the rest energy of an electron (1022 keV):

$$\sigma^2 = d^2 + k(E_\gamma - 2m_0c^2) \quad (9)$$

The value for the inherent electronic noise component of broadening is independent of the mode of operation as is the proportionality constant.

These two relations are used in the same manner as are the two relations for efficiency, equations (6) and (7), i. e., equation (8) is used with equation (6) for gamma energies less than or equal to 2800 keV and equation (9) is used with equation (7) for gamma energies greater than 2800 keV. The two constants in equations (8) and (9) are determined by measuring the resolution in keV at two different gamma energies and become input parameters in the program.

The program can be used to calculate and plot the spectrum using instantaneous activity or activity integrated over an specified time interval. That is, it has the capability of determining activities at several times, summing these activities, and plotting the resulting spectrum as that representing the average spectrum taken over a specified counting period. It was thought that in order to obtain accurate spectra in the actual experiment counting times short compared to the time after fission would be needed. By using the integration capability of the program it was possible to predict that practically no change would be observed in the shape of the spectra when an instantaneous spectrum was compared with one in which the counting period was approximately 50% of the average time after fission.

After every gamma activity has been calculated and assigned to a proper element of the one-dimensional spectrum matrix, the elements are added to give a total gamma "activity". This value is not the value of the gamma activity emitted by the sample at the

particular time of observation but rather the total activity detected by the simulated detector. It has been corrected for detector efficiency and all elements are considered normalized for sample size and neutron flux, i. e., divided by the value $\Sigma_f \phi$. The relationship between this total detected activity and time after instantaneous fission should be similar to that observed by Hunter and Ballou [24] and, where the times overlap, to the work of Perkins and King [7]. Although the shape of the total detected-activity versus time-after-fission curve is not really a true representation due to the efficiency weighting, there are basic similarities between the relationship calculated by the program and the work cited above.

There is also a provision in the program for a listing of each fission product isotopic activity normalized for sample size and neutron flux, at any particular time after instantaneous fission. This is isotopic activity and is completely independent of the number and energies of its gamma rays, if any are associated with that fission product and independent of the detector parameters. The growth and decay of each individual fission product could be observed as was done by Clark [14] and Faller, Chapman and West [25].

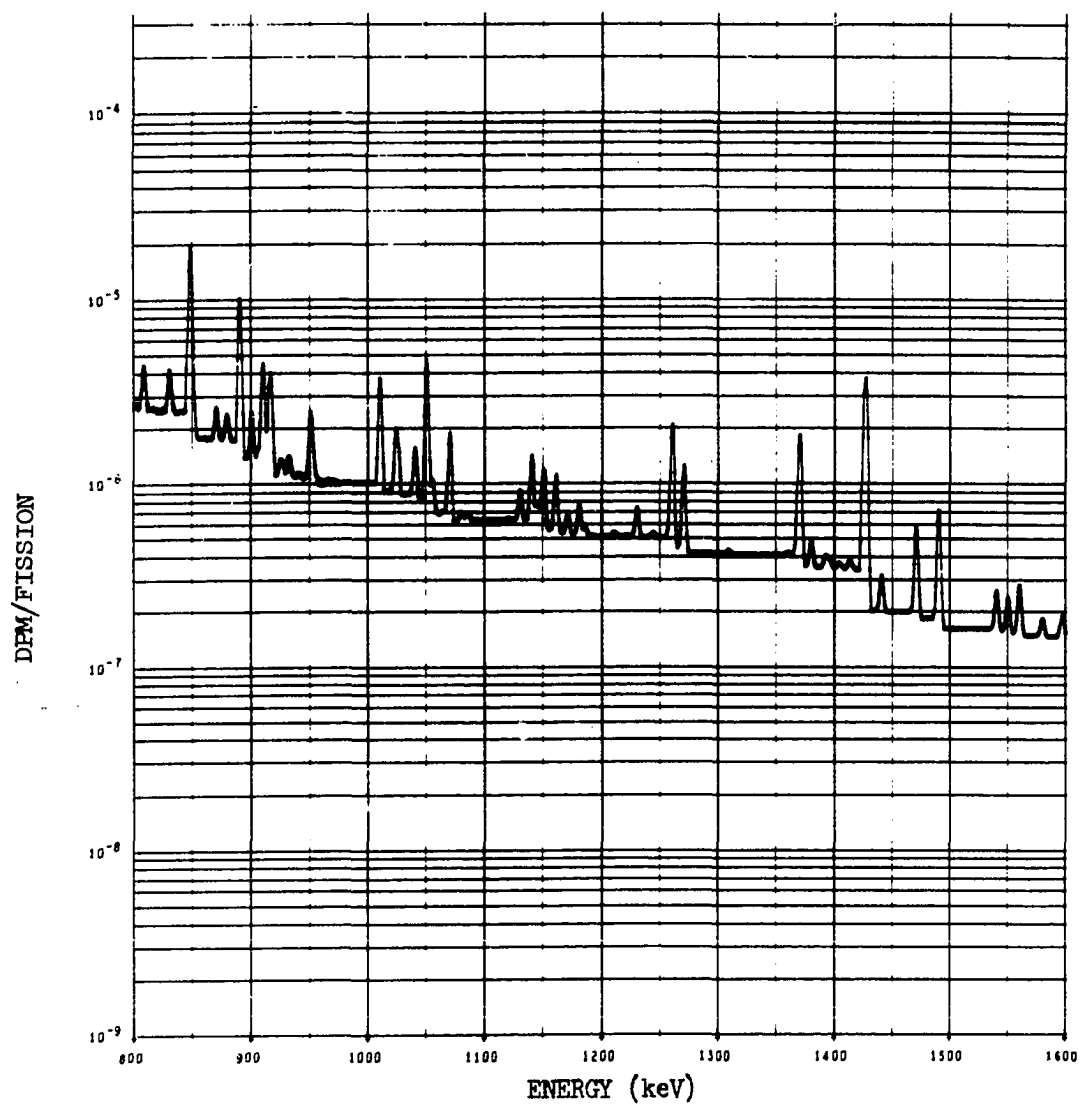
In conjunction with the listing of the isotopic activity there is also a listing of the detected activities of each gamma ray of the particular fission product in question. These activities are simply the isotopic activity multiplied by the particular branching ratio of the gamma ray and corrected for detector efficiency, and therefore do not represent the true gamma activity emitted by the fission product. This provision was introduced to determine the

relative detected activities that two or more gamma rays of the same energy contribute to a single peak at that energy. The information gained from this provision can be used to obtain good estimates of the relative contributions of gamma rays in the matching peaks of the actual experimental spectra.

This computer program was devised to simulate one particular problem: the observation of fission product gamma ray spectra as a function of time after instantaneous fission. However, with only minor changes, the program can be modified to plot the spectra of the more practical case of continuous production and shutdown of a reactor. These changes involve only a small part of the Bateman equations, as a comparison of equation (3) with equation (4) will show. This would give spectra dependent on two parameters instead of just one, i. e., not only time after fission, t , shutdown, but also time of operation, T , production. Of course, the batch decay set, equation (3), could also be easily replaced by the continuous production set, equation (1). The results of these calculations would be extremely interesting. The gamma spectra would depict each fission product's approach to equilibrium concentration. A provision could easily be added to this particular program that would calculate the per cent saturation of each fission product at any time after the start of production. This could be done by finding the concentration of each fission product after an infinite period of production and then comparing this value with the concentration calculated at the period of interest. The spectra from the continuous production program could not be considered a simulation or prediction of what actually would be observed through

the detector. The fission product gamma spectra would be predicted as accurately as the data are known, but there is no provision in this program for the insertion of the fission gamma ray peaks into the spectra. This could be done with the known fission gamma energies, their per cent occurrence per fission, and the rate of fission and then by calculating a fission gamma "activity" and assigning it to its proper location in the spectrum matrix.

A sample spectrum from calculations using the batch decay set of Bateman equations appears in Figure 2.



PREDICTED SPECTRUM AT 52 MINUTES AFTER FISSION

FIGURE 2

CHAPTER IV

EXPERIMENTAL PROCEDURE AND EQUIPMENT

In order to observe the fission product gamma ray spectra at short times after fission, an almost completely automatic procedure has been used. Automatic operation was necessary for several reasons. At these short times the starting, stopping, and various other manipulations of the detection system necessarily occur in such a rapid sequence that they cannot be done manually. In addition, the many sample cycles required to obtain good statistical data require the use of electronically controlled sample handling to insure reproducibility.

A small strip of oralloy foil (uranium enriched to 93.5% U^{235}), contained in a nylon "rabbit", is inserted into the thermal column of the Omega West Reactor. The rabbit is pneumatically propelled through a shuttle tube by means of helium gas under high pressure. After a short period of irradiation the gas flow is reversed so that the rabbit travels back through the tube until it is positioned at the terminal end in front of the germanium lithium-drifted detector. Prior to the arrival of the irradiated sample at the terminal end, a 1600 channel pulse height analyzer is started and accumulates pulses in the first 200 channel subgroup. The analyzer is programmed so that each 200 channel subgroup will accept pulses over the same energy

increment at successively longer times after fission and successively longer counting periods. When the rabbit arrives at the terminal end, a pulser is started which drives eight binary scalers, one for each analyzer subgroup. For a specified number of counts in each scaler the appropriate subgroup accepts pulses from the detector. Thus, the scalers are timers and at specified times the analyzer switches to the next subgroup until the analyzer is storing pulses in the last subgroup. When the last scaler has counted its specified number of counts, the analyzer is disabled and the storing of pulses will cease. This occurs at about 45 seconds after the arrival of the rabbit at the terminal end. The pulser is then stopped and the scalers are reset to zero counts. Resetting the scalers automatically resets the analyzer program board to store in the first subgroup again. The irradiated sample is replaced by a fresh sample or one that has cooled for several minutes after short irradiation. This changing of samples is intended to guard against the buildup of longer-lived fission products.

This procedure is repeated several times with each run's detector pulses being added onto the counts already stored in the analyzer. this is done until enough counts have been accumulated to insure good statistics in each spectral set. The eight spectra are then read out and stored on paper tape for future analysis. The analyzer memory is then zeroed and the bias level of the energy increment is advanced to the upper limit of the previous energy increment and the time-dependent spectra are obtained for this new higher-energy increment in the same manner as before. This sequence of operations is repeated until the observation of fission product gamma rays is completed, somewhere

around 1 MeV. (Data of higher energies were not taken due to the statistical deterioration of the spectra.) The paper tapes now contain the full-energy (0-1.1 MeV) spectra for eight different times after fission with the longest time being about 31 seconds after fission.

The timing pulser is now altered to emit pulses at a slower rate. This drives the scalars at a slower rate and enables the subgroups to be switched after longer counting periods, and thus, longer average times after fission. In this case there is about a 40 second delay between the time the rabbit is positioned and the starting of the analyzer. The eight average times after fission for this latter sequence range from one minute to approximately two hours. The samples are irradiated for a slightly longer period for a higher counting rate at the longer times.

Because the target of U^{235} is extracted and positioned in such a short time after fission most of the delayed neutron precursors will not have had time to decay. The target sample can be expected to emit almost the entire delayed fraction (.0064) of total fission neutrons while positioned in front of the detector. If a significant number of delayed neutrons is detected then the fission product spectra will show components from this contribution. The most probable interaction of these neutrons with the germanium detector is inelastic scattering [26]. The dominant peak would be at 691 keV arising from the production of the 0+ first excited state of Ge^{72} . This state can decay only by electric-monopole conversion electrons which are detected with 100% efficiency. The peak would appear at the full transition energy because the energies of the conversion electron and subsequent X-rays are summed in the detector and both are detected with ~ 100% efficiency.

The cross section for the production of this state is about 80 mb.

Other peaks arise from gamma rays produced by inelastic neutron scattering from the germanium isotopes in the detector, Ge^{70} , Ge^{72} , Ge^{73} , Ge^{74} , and Ge^{76} .

Calculations show that during the counting period one sample will emit 6×10^7 delayed neutrons (89% of total delayed emission) after a one second irradiation. However, only 10^3 of these will reach the detector when the solid angle is considered. This number is actually too large since it considers no material between detector and sample when, in fact, there will be 1/4 inch of acrylic resin (structural material for the terminal piece) in addition to small thicknesses of quartz, nylon, and aluminum between the detector and the sample. Considering the cross section stated above for the predominant interaction it was determined that only about 11 interactions would be detected by the analyzer over the entire time span of 42 minutes. The highest number of counts, 4, would occur in the seventh subgroup. Assuming the gaussian distribution less than one count would appear in the peak channel per sample.

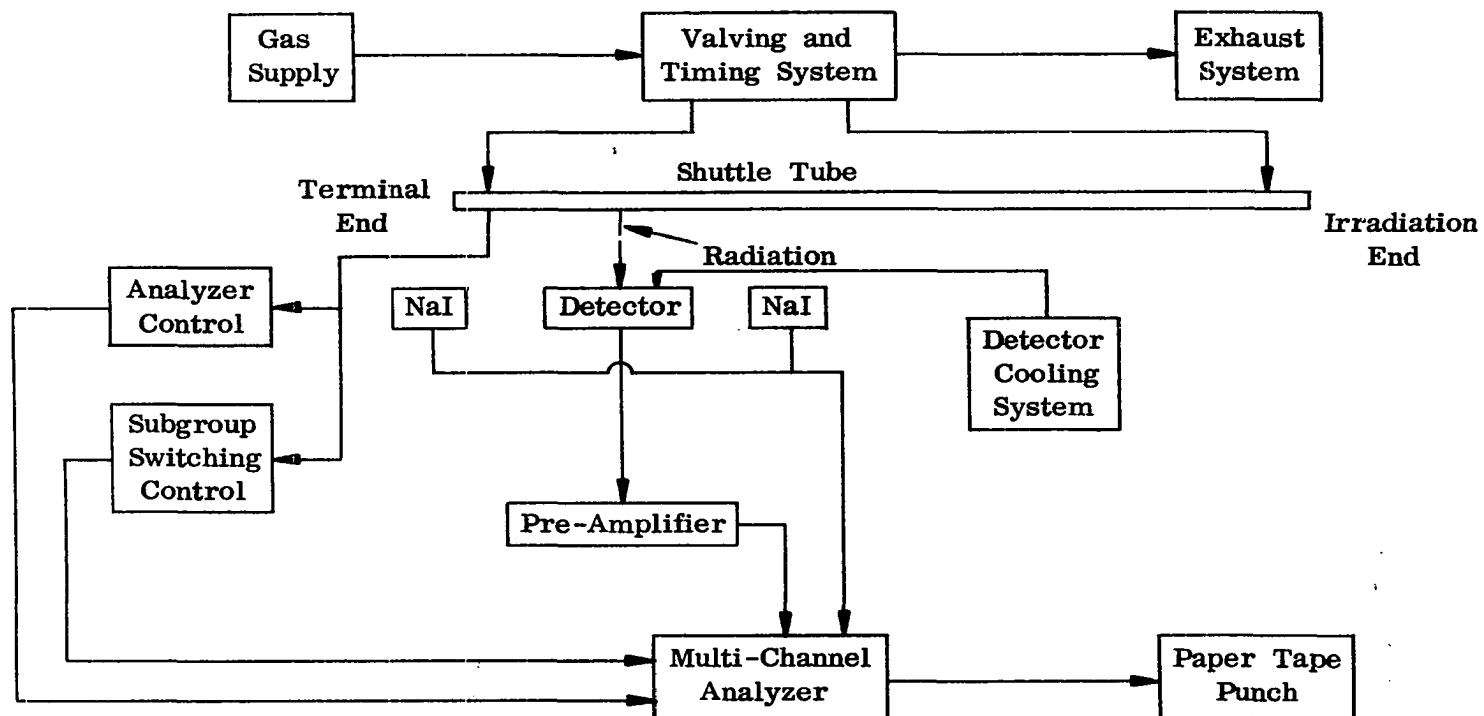
In the case of the longer time spans the irradiation time is increased by about a factor of ten, thereby increasing the number of delayed neutrons emitted by a factor of ten. However, since there is a wait time of about 40 seconds before the accumulation of pulses, essentially all the delayed neutron precursors will have decayed. Thus one can neglect the possibility of delayed neutron contributions.

The equipment required for sample handling and data acquisition consists of the interconnection of several complex components. Each of these components will be considered and explained in detail. A block

diagram of the interconnection of the experimental equipment appears in Figure 3.

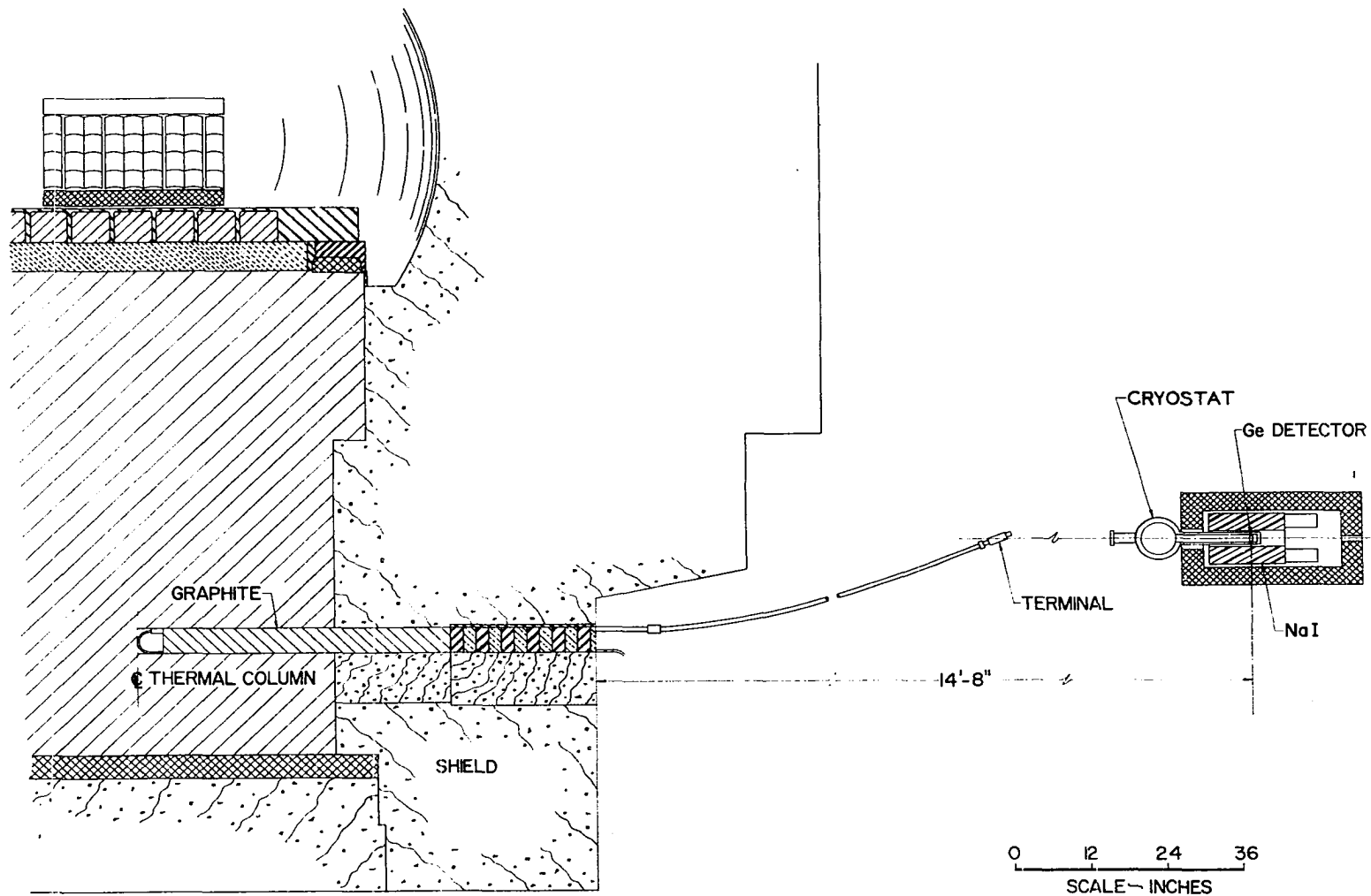
The target sample must be brought out of the reactor thermal column as rapidly as possible. This necessitates having the rabbit travel over as short a distance as practicable to reach the detector. The port that was chosen for sample insertion was TC8-N on the north side of the thermal column of the Omega West Reactor. The location of this port relative to the rest of the reactor system and the detection system is shown in Figure 4. This port measures $12 \frac{3}{4}$ inches by $12 \frac{3}{4}$ inches and extends all the way through the graphite thermal column and concrete shielding. It contains a 3 by 3 array of graphite stringers and shielding plugs. The pneumatic system is positioned in the upper-right-most location. The flux at this position (85 inches from the core centerline) is 3.6×10^{10} neutrons/cm²-second at full power (5 megawatts).

The right-most stringer and shield plug of the top row were removed and replaced by a grooved stringer and a grooved shield plug. The stringer and plug were grooved on opposite sides to accept the tubing of the shuttle system. The shuttle tube which carries the rabbit was placed in the groove nearest the core. This tube measures $\frac{1}{2}$ inch internal diameter. In the opposite groove was placed the gas tube measuring $\frac{1}{4}$ inch outside diameter. The gas tube is welded to the shuttle tube at the centerline of the thermal column and has a U-bend at that point so it will fit in the groove opposite the shuttle tube. This gas tube acts as an exhaust line when the rabbit is inserted and a pressure line when the rabbit is extracted. The grooves were



BLOCK DIAGRAM OF DATA ACQUISITION EQUIPMENT

FIGURE 3



PLAN VIEW OF EXPERIMENT
FIGURE 4

formed in such a way as to prevent the direct streaming of neutrons out into the working area. Aluminum was chosen as the structural material since it is easily formed and will withstand the temperatures in the thermal column. On extraction, after the rabbit reaches the edge of the concrete shield, it must travel about 16 inches in the transverse direction and down about 6 inches over a floor length of 12 feet to reach a suitable position in front of the detector. To assist in proper positioning at the terminal end the shuttle tube arcs up then down with the maximum of the arc being about two feet above the detector. The rabbit is then in a final position at an angle of approximately 45 degrees with respect to the floor. Polyethylene tubing of the same size as the aluminum tubing was chosen for this segment of the system.

The counting system must be "informed" when the rabbit arrives at its terminal position so a special terminal piece of tubing must be designed and built to perform three functions: (1) act as an "informer" at the arrival of the rabbit, (2) have the capability to be detached from the system so that a sample change can be made, and (3) act as a gas exhaust as well as a gas pressure inlet. When the rabbit arrives at the end of the transfer tube, an electrical contact is made allowing a signal to be brought out from the system. The upper part of the terminal piece is divided and joined by a threaded coupling to allow sample change. A gas nozzle is inserted in the lower end to serve as either a gas inlet or outlet. This terminal piece is made of clear acrylic resin of the same size as the polyethylene and aluminum tubing.

A valving and timing system controls the driving of the rabbit to insure reproducibility. Two three-way solenoid operated valves are used with each being assigned to an end of the shuttle system. They must be operated such that when one is in the exhaust position the other is in the gas inlet position. Three different timers are used. One determines how long the gas stays on to drive the rabbit into the thermal column, another determines the length of time the rabbit will be irradiated and when to start the exhaust, and the final one determines how long the gas that drives the rabbit out stays on. The timing system is flexible enough to allow irradiation times and gas pressure times of up to 15 seconds.

Because the rabbit moves at great speed the gas must be left on for a longer time than the transit time to avoid bouncing. Maintaining gas pressure after the rabbit has reached the end of the tube will tend to hold it there. This is not so much a problem during the irradiation part of a cycle since the rabbit must travel through thirty inches of thermal column before reaching the tube end at the centerline of the thermal column. The flux along the tube is essentially constant and any bouncing will not appreciably affect the number of fissions. The problem could be serious at the terminal end, however, since the detector offers a small area to the gamma rays and is positioned about two feet down a tube and five feet from the sample. Once the rabbit has been positioned in front of the detector any transverse or vertical movement will prevent the gamma rays from having a direct path to the detector. For this reason gas pressure must be maintained for a slightly longer time after the rabbit has hit the contacts. This timing system is fairly flexible

allowing irradiation times and gas pressure times of up to 15 seconds.

The rabbit should be brought out of the reactor as quickly as possible. The main force opposing the rabbit on exit is the gas it must push out in front of it. A system was constructed so that this exhaust gas could be dumped into a ballast tank which is continuously being pumped. The shuttle tube is opened to the ballast tank when the exit gas pressure driving the rabbit out is applied. This system results in an improvement of about 200 msec over the system with no ballast tank. At 20 psig the rabbit can be brought out and positioned in front of the detector in 600 msec. However, the time of interest is the time after fission or the time after the rabbit is brought from the flux of neutrons. The rabbit must travel the first two and one-half feet of the eighteen foot path while still in the thermal column. Approximate calculations indicate that the rabbit travels for 200 msec before leaving the neutron flux. This gives a time after fission upon arrival at the terminal of 400 msec. This transit time was used as standard for all analysis.

The ~ 100 mg or alloy target foils were purposely made thin to avoid as much self-shielding as possible. At the irradiation position in the shuttle tube a sample will undergo 5×10^9 fissions/second. The foils were doubly contained for insurance against fission gas release. The foil is first sealed in quartz tubing which has a 1 millimeter thick wall, an outside diameter of 8.5 millimeters and a length of 25 millimeters. The sealed foil is then placed in a standard OWR rabbit, a nylon cylinder with a polyethylene cap. Quartz wool is packed on both sides of the

quartz tube within the rabbit to cushion the inner container upon impact. Because of the several bends in the shuttle tube the rabbit outside diameter had to be reduced to insure easy passage.

Thirteen samples were used, thereby allowing each sample approximately thirty minutes cooling before its reuse. This is sufficient to allow almost all the fission products produced during the short irradiation time to decay to insignificant activity. In addition to the thirteen target samples one dummy was prepared. This is a sealed quartz tube containing no or alloy and packed in a standard nylon rabbit. The purpose of this rabbit is to determine background levels and to provide a non-radioactive rider to check the pneumatic system.

The high number of fissions and the short transit time out of the neutron flux tend to make the sample a radiological health concern. After a one second irradiation the sample upon arrival at the terminal position has a contact exposure rate in excess of 5 rem/hour, beta plus gamma. Even though the activity drops rapidly the high number of manual sample changes necessitates some safety procedures to cut down the extremity exposure. The sample is allowed to cool for a moderate length of time after completion of counting before the sample is changed. Also, the sample is dropped into a funnel and tube arrangement which transfers the sample by gravity into a lead pig, thereby cutting down the handling time.

As was mentioned earlier, it is necessary that a large capacity multi-channel analyzer be available for the storage of the detector pulses. This need is satisfied with the SCIPP (Silicon Computing

Instrument - Patch Programmed) 1600 built by the Tullamore Division of Victoreen. This analyzer has a capacity of 1600 channels for storage and is of standard design in its function of sorting pulses of different heights into their respective energy slots or channels.

From the standpoint of observing time-dependent fission product gamma ray spectra the advantage in this analyzer is not that a large energy span could be used, but that the 1600 channels can be divided into equal subgroups with each subgroup representing a particular time after fission. In this problem eight 200-channel subgroups are used. For a particular 200-channel energy increment, one run through the analyzer memory yields eight spectra. Because of the rapid decay of gamma activity, each successive subgroup must be available for storage for succeeding longer periods of time. Each subgroup is available approximately twice as long as the preceding subgroup. This means that each spectrum will be that representing the gamma activity for an average time after fission of twice the time after fission of the preceding spectrum.

Since only 200 channels are available for each spectrum, a somewhat limited energy increment was necessary. The energy spread was selected on the basis of the resolution attainable at the average energy of the increment. At low energies the resolution is quite good (around 3 keV, fwhm). Three channels are sufficient to identify the peak energy so with the first energy increment a proportionality factor of about 1.5 keV per channel allows enough channels

per peak such that the normal resolution could be utilized. However, as the energy of observation increases, more channels are used per peak due to the broadening of the peaks. The proportionality factor can, therefore, increase with each energy increment. It should also be noted that at high energies (greater than 1 MeV) the spectrum is not as densely populated with gamma rays as is the lower energy spectrum. For this reason the decrease in resolution of the detector does not seriously impair the ability to identify the individual gamma rays.

The analyzer is physically separated from the pneumatic system by several rooms and a distance of about 100 feet. This necessitates some type of remote control to not only start the analyzer accumulating and then to finally disable it but also to switch the subgroups at the proper instant. This problem is simplified in that all electronic commands in the SCIPP are made by grounding the proper pin or location in the circuitry. By bringing out the analyzer ground wire and a wire from the point that bypasses the accumulate pushbutton and by connecting both to a microswitch, a remote accumulate switch becomes available. Closing the switch will cause the accumulate flip-flop circuit to be reversed and the analyzer will start storing pulses and continue to do so until the disable switch is closed. Because of a time delay of about 0.3 second between the time the accumulate switch is closed and the actual start of accumulation, the accumulate switch is closed manually while the rabbit is in the thermal column.

A system for switching the storage locations at the proper instant has also been developed. After the counting period in each subgroup has ended no attempt was made to disable the analyzer.

The switching was done while the analyzer was storing. There was no problem involved since the switching could be accomplished in a few microseconds. The particular subgroup that is to receive pulses is determined by whether or not certain locations in the address circuit board are at ground potential. For the purposes of this experiment only three such locations are of interest. These three locations are conveniently duplicated by pins located on the front of two of the address boards. Each successive subgroup is available for storage by grounding the pins in binary order, i. e., no pins grounded opens the first subgroup, pin 1 grounded opens the second subgroup and disables the first, pin 2 grounded opens the third subgroup while the first two are disabled, grounding pins 1 and 2 opens the fourth subgroup, and so on until the eighth subgroup is opened by grounding all three pins. These pins are connected to remote positions at the pneumatic system. There are now six remote contacts at the pneumatic system site: three for memory location, one for the accumulate bypass, one for the disable bypass, and one for the analyzer ground.

The timing system for subgroup switching is initiated when the rabbit closes the terminal contacts, starting a pulsing scaler. This scaler emits 12 pulses every second which are of sufficient height to drive eight binary scalars. These scalars act as the timers for determining how long each subgroup will accumulate data. A change in voltage is obtained at preselected times causing a transistor to conduct energizing a mercury relay. The energizing of the relay does two things: the scaler is turned off to prevent the same time pulse

from appearing again and a pulse is produced which drives a ninth scaler. The ninth scaler receives a pulse every time a scaler is turned off thus acting as a binary counter and converter for the analyzer subgroups. Each of the first three binary stages of this scaler is connected to a mercury relay through a transistor and thus acts as an analog for each of the three address pins in the analyzer memory. In cases when two or more binary stages determine a switching time a diode coincidence "and" circuit is used. The eighth scaler, of course, will not switch to a new subgroup but, instead, its relay will ground the disable bypass contact shutting off the analyzer.

The development of Ge(Li) spectrometry techniques was the main factor in determining that this experiment could and should be done. As was mentioned earlier almost the entire work that was previously done in observing fission product gamma ray activity was done with limited resolution sodium iodide crystals. Now that solid-state detectors are available, the work can be performed with high precision in determining the energies and half-lives of individual gamma rays that are observed. Data were taken with a lithium-drifted germanium diode having a depletion layer of 3 millimeters and a 2 cm^2 area. The small volume of this detector was not serious since the source strength was high.

High resolution lithium-drifted germanium gamma ray detectors have a large Compton continuum in their pulse height distributions. This is due to their small dimensions and low atomic number. The detector used here has been combined with a large annular NaI crystal, which is used to suppress the Compton distribution but does not seriously

reduce the number of pulses in the full-energy peak. If a gamma ray beam is incident on the semiconductor, a certain number of interactions will occur in which the gamma rays are completely absorbed. However, many of the gamma rays undergo a Compton scattering and lose only part of their energy in the semiconductor. There is always a scattered gamma ray associated with this process, and detection of this scattered gamma ray provides a means of identifying Compton events. Since the large NaI crystal has a high probability of absorbing all or part of the energy in the scattered gamma ray, a second pulse is usually generated in coincidence with the pulse from the semiconductor. When this time coincidence occurs, it is assumed that the detector pulse was due to a Compton event and it is discarded by an anti-coincidence circuit. This technique is particularly effective for gamma rays of energy between 0.3 MeV and 2.0 MeV. At energies below 0.3 MeV the photo-electric cross section is high, and there is not a large Compton distribution. At energies greater than 2 MeV the pair production cross section is large and double or triple coincidence techniques can be used to enhance the double escape peak.

At energies greater than 2 MeV pulses from the NaI crystal are amplified and sent through a single channel analyzer which is gated such that only those pulses which have an energy equal to twice the rest mass energy of an electron (1022 keV) are allowed. When such a pulse is detected in coincidence with a pulse from the semiconductor then the semiconductor pulse is assumed to be the double escape pulse ($E_\gamma - 1022 \text{ keV}$) and is allowed through to the multi-channel analyzer to be stored. Semiconductor pulses not in coincidence with the 1022

keV NaI pulses are discarded.

The detector is cooled to liquid nitrogen temperature by conduction down a hollow aluminum "cold finger" inside a Dewar. The detector must be kept cold to stabilize the lithium atoms in the Ge lattice. Without proper compensation with lithium, the detector characteristics deteriorate greatly. All of the structural materials inside or near the detector have been designed to minimize scatter and absorption of the gamma rays. A vacuum is maintained in the "cold finger" to insure cryogenic insulation.

CHAPTER V

DATA REDUCTION AND EXPERIMENTAL RESULTS

The fission product spectra are extremely complicated due to the growth and decay of many fission products and their associated gamma rays, particularly during the observation times shortly after fission. Since the identification of the many gamma rays contributing to the peaks would be difficult and inaccurate by direct observation, a least squares fitting program called NAL was applied to the individual gamma rays forming the spectrum. The data were fitted to the function

$$Y_i = \frac{A}{\sqrt{2\pi}} \cdot \frac{1}{\sigma} \cdot e^{-\frac{1}{2}(\xi^2/\sigma^2)} + C \cdot A \cdot e^{-D\xi} \left[1 - e^{-\frac{1}{2}(\xi G)^2} \right] \quad (10)$$

$$Y = \sum_{i=1}^{JJ} Y_i + B \quad (11)$$

where:

$$\xi = Z - E_i$$

= the interval in energy between the energy being considered,

Z, and the centroid, or peak energy, E_i , of the i-th peak

Y_i = number of counts at the energy being considered, Z, of the
i-th peak

A = the area of the peak

σ = the gaussian width of the peak

C = the extrapolated exponential tail amplitude at the gaussian peak

D = the slope of the exponential tail

G = the gaussian tail cut-off width control

JJ = the number of peaks being fitted - 8 maximum

B = the background

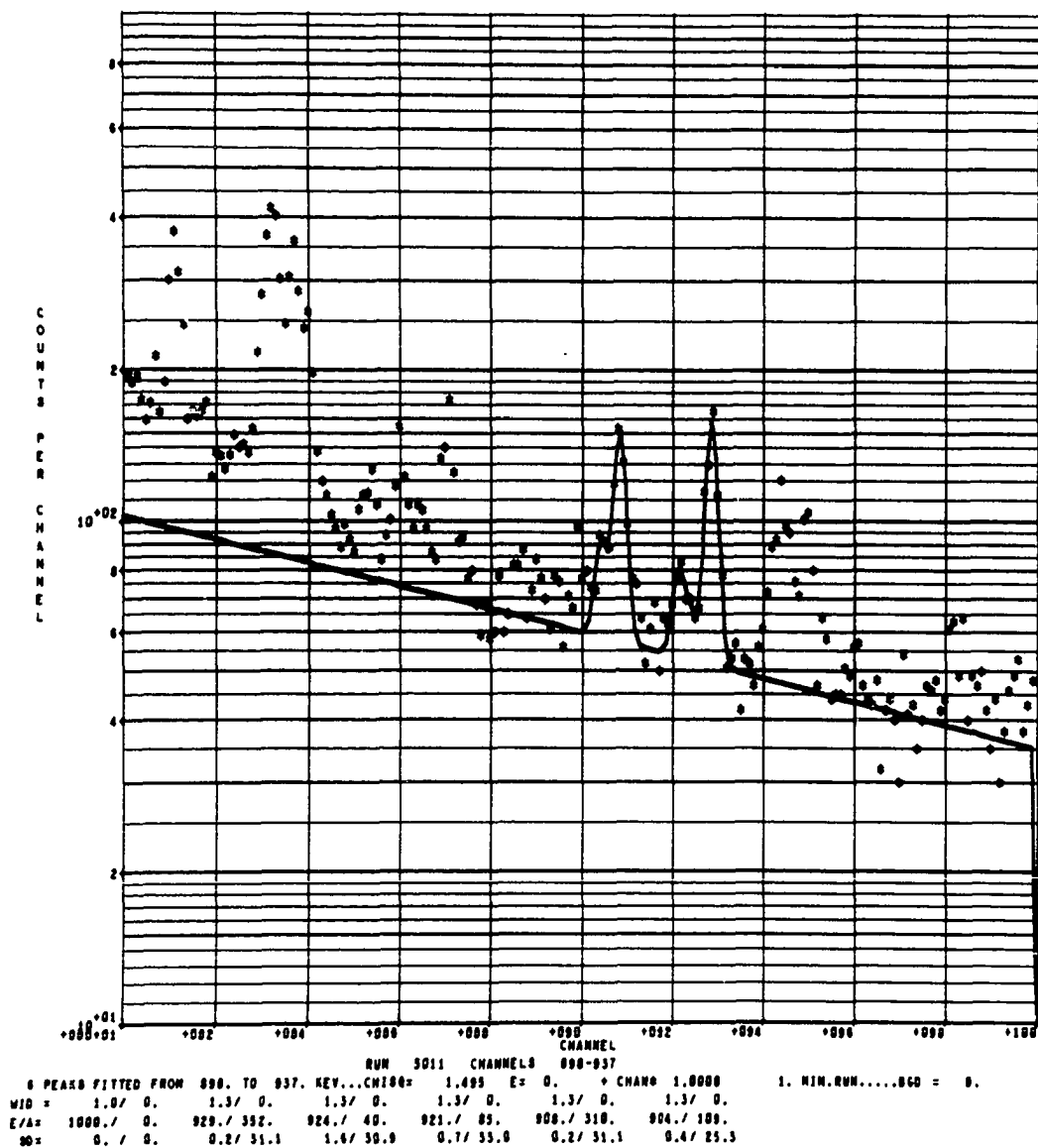
The function is a gaussian distribution with an added exponential left-hand tail which goes to zero smoothly at the centroid of the gaussian peak. The gaussian function closely represents the response of a solid state detector to an incident gamma ray. The parameters of this function are σ , E, A, C, and D. The gaussian tail cut-off width control, G, which determines how sharply the tail breaks off under the peak, the background, and the number of peaks being fitted are constants which are read into the program and not computed. Because of the complexity of the spectra, only the centroid and the area were allowed to vary to provide a fit. The width was fixed at a value determined from calibration runs in which the width was allowed to vary, in addition to the centroid and the area. The "tail" part of the function was used to fit backgrounds with a simple exponential by introducing a dummy peak having vanishingly small area. Thus C and D became background parameters. This procedure left seven real peaks available for fitting. Since each data subgroup rarely contained only seven peaks, several fittings had to be made over each subgroup.

The fittings were performed on an IBM 7094 Computer which allows three forms of output for NAL. The final values of the

parameters are punched on output cards with the same format as the input initial estimate cards so that the results can be used as initial estimates on any succeeding fitting if so desired. A print-out is also made of the final values of all parameters along with the initial estimates of those parameters and the standard deviations of all parameters that are allowed to vary. In addition, a plot is made on 35mm film of the fitted function superimposed on the actual data. A sample of this film output appears in Fig. 5.

As stated previously, thirteen or alloy target samples were used with masses ranging from 84 to 142 mg. The average mass was 111.3 mg. The neutron flux at the irradiation position inside the graphite thermal column was 3.6×10^{10} neutrons/cm²-sec.

Three different irradiation times were used. For data ranging from 0.4 second to 42 seconds after fission an irradiation time of approximately 0.5 second was used. This was the shortest irradiation time achievable since the rabbit traveled for 200 msec going into and 200 msec coming out of the thermal column, thus totaling 400 msec irradiation while traveling. An estimate of 100 msec was made for the time required for solenoid valve reversing, thus giving a total of 500 msec. With the counting position five feet away from the detector, the total pulse rate from the detector registered 1100 counts per second, and a count rate higher than this would have distorted the peak shape. For the longer counting times ranging from 0.7 minute to 152 minutes higher irradiation times were used and data were taken from 5 keV to 750 keV with a 6.4 second irradiation. Since there was a wait time of 0.7 minute before the



Sample Output of Fitting Program

Figure 5

analyzer was started, the count rate from the detector had decayed to 1100 counts per second. For the highest energy increment, 750 keV to 1130 keV, the pulse rate reaching the analyzer was low so an increase in irradiation time to 9.0 seconds was utilized. Even though this higher irradiation time increased the detector response rate to 1400 counts per second at 0.7 minute after fission, the peak shape was not distorted because of the use of a blocking circuit.

As was mentioned in Chapter IV, each analyzer subgroup was allowed to accept pulses for a period approximately twice as long as that of the preceding subgroup. The counting intervals and approximate mean times for each analyzer subgroup are tabulated in Table 1.

The intrinsic efficiency decreases very sharply with energy for gamma rays of energies less than 2 MeV. For this reason many samples had to be counted at the higher energy increments to obtain enough counts per channel, thus insuring adequate statistical accuracy for fitting purposes. The number of samples counted for each energy increment for both the short and long times are tabulated in Table 2 along with the irradiation times for each increment.

Correction for analyzer dead time was not significant. For a 200-channel subgroup the average resolving time for the SCIPP 1600 is approximately 25 μ sec. Even at the highest observed pulse rate entering the analyzer the correction was less than 3 per cent. It has been found necessary, however, to provide a separate blocking circuit to inhibit the analyzer after each pulse stored because of amplifier baseline instabilities. The effect of these instabilities is to distort the line response shape. At very high counting rates

TABLE 1

COUNTING INTERVALS AND MEAN TIMES FOR THE ANALYZER SUBGROUPS

| Analyzer Subgroup | Counting Intervals | | Mean Times | |
|-------------------|--------------------|------------------|-------------------|------------------|
| | Short Times (sec) | Long Times (min) | Short Times (sec) | Long Times (min) |
| 1 | 0.4 0.57 | 0.7 - 1.3 | .5 | 1.0 |
| 2 | 0.57 - 0.90 | 1.3 - 2.5 | .7 | 1.9 |
| 3 | 0.90 - 1.57 | 2.5 - 4.9 | 1.2 | 3.7 |
| 4 | 1.57 - 2.90 | 4.9 - 9.7 | 2.2 | 7.3 |
| 5 | 2.9 - 4.6 | 9.7 - 19.7 | 3.7 | 14.7 |
| 6 | 4.6 - 9.6 | 19.7 - 38.7 | 7.1 | 29.2 |
| 7 | 9.6 - 21.2 | 38.7 - 76.7 | 15.4 | 57.7 |
| 8 | 21.2 - 42.0 | 76.7 - 152.7 | 31.6 | 114.7 |

TABLE 2

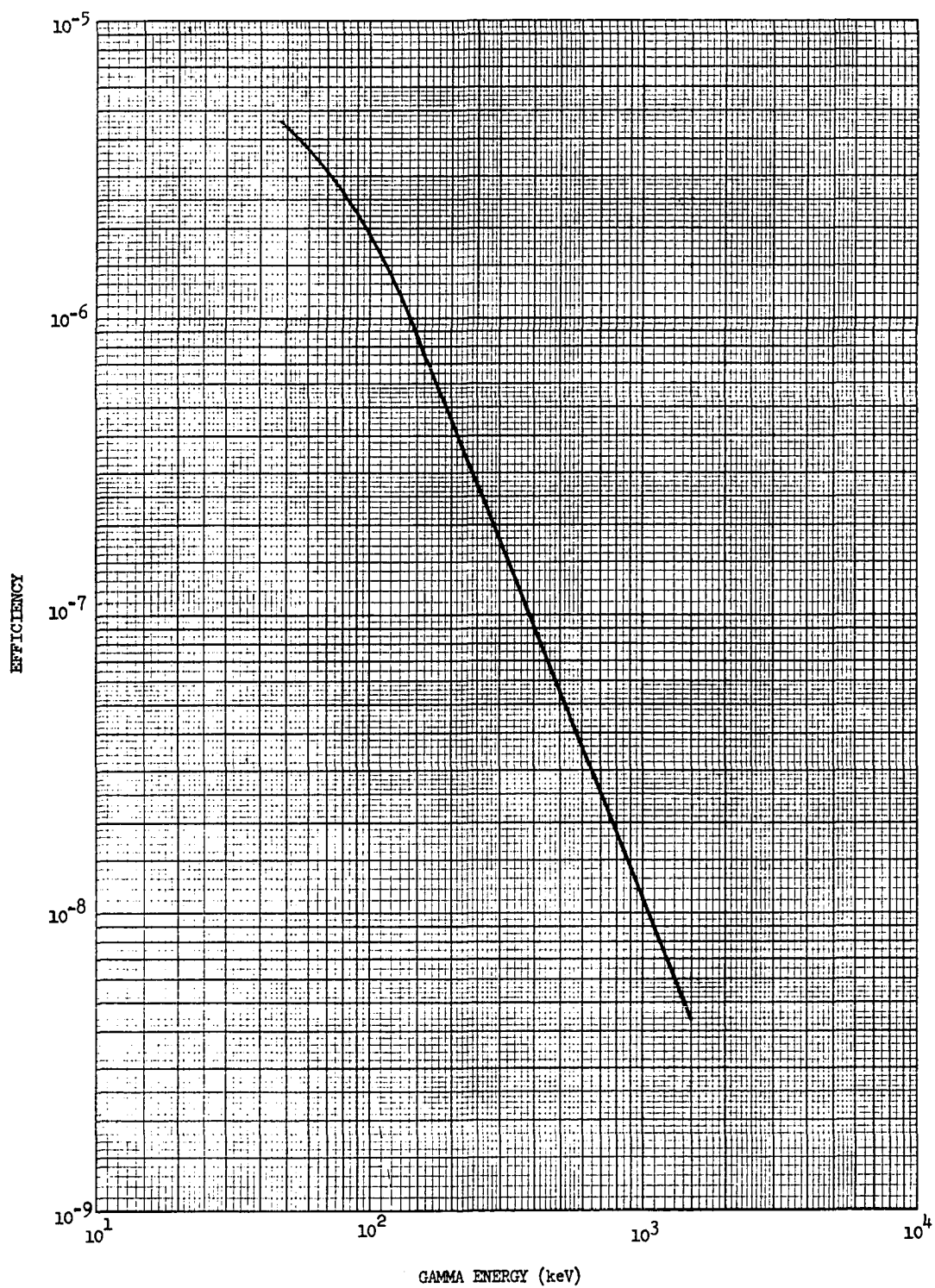
IRRADIATION TIMES AND NUMBER OF SAMPLES
FOR THE ENERGY INCREMENTS

| Energy Increment (keV) | Irradiation Times (sec) | | Number of Samples | |
|------------------------|-------------------------|------------|-------------------|------------|
| | Short Times | Long Times | Short Times | Long Times |
| 5-287 | 0.5 | 6.4 | 268 | 5 |
| 262-530 | 0.5 | 6.4 | 325 | 19 |
| 500-760 | 0.5 | 6.4 | 650 | 43 |
| 750-1130 | 0.5 | 9.0 | 1300 | 74 |

this effect can be disastrous. When the blocking system is in operation, a blocking signal will override the gating signal after each data pulse and hold the analyzer closed for 200 μ sec. The per cent blocking time is, therefore, similar to per cent dead time and varies linearly with the detector response rate with a value of approximately 17 per cent at 1000 counts per second. Blocking time corrections varied from as much as 20 per cent for the first subgroup of the 750 to 1130 keV energy increment to 3 per cent for the third subgroup of the lower energy increments.

The relative efficiency of the detector was determined by using several radioisotopes of known activity and absolute efficiency was determined by irradiating a gold foil and counting with the foil in the same position as the target samples. The efficiency of the detector was quite small due to the small solid angle subtended from the counting position five feet away. The net efficiency curve for the detector is shown in Fig. 6.

There was essentially no interference caused by background radiation. For the short time observations background was negligible compared to the activity of the target sample. At the longer times, background contribution was less than 10% of the total spectrum due mainly to the lead shielding around the outside of the NaI annulus. However, there was a contribution from an internal source. A slight amount of Na²² contamination has been observed within the detection system so that for the long counting times the annihilation peak at 511 keV will always be present. Calculations show that delayed neutrons did not contribute to the background and experimental verification of



EFFICIENCY OF DETECTOR

FIGURE 6

these calculations was obtained by observing a Pu-Be neutron source for several hours. There was nothing evident in the normal background spectrum to indicate that there was a contribution from neutrons.

Self-absorption is another factor that was taken into consideration at low energies. Uranium is dense and even though a thin foil was used self-absorption was considerable at energies below 100 keV. Because of its length the sample foil was folded twice giving the effect of a foil approximately four mils thick. Self-absorption ranged from as much as 67 per cent at 50 keV to 8 per cent at 200 keV to less than 1 per cent at 400 keV.

Resolution for Ce^{139} (165.8 keV) was 3.4 keV (2.0 per cent) full width half maximum. At the highest calibration energy, 1115.6 keV (Zn^{65}), the resolution was 4.3 keV (0.4 per cent). Although some of the data were accumulated over periods of several days with one particular energy increment requiring two weeks the electronics remained stable. No bias drift or gain shift was evident.

Results of the computer fittings are tabulated in Table 3 and Table 4. The least squares peak channel was converted to peak energy by values obtained from the calibration runs for that particular energy increment. The standard deviation of the peak energy was statistically computed from the known standard deviation of the peak channel and the computed error of the channel-energy conversion constant. Using the parameters mentioned above the gamma activity for each analyzer subgroup was calculated in units of disintegrations per minute normalized for a one-sample observation and a one-second irradiation. Since the average mass of the samples and the flux are

known, these activities can be converted to disintegrations per minute per fission. Some approximate half-lives were determined and listed along with the gamma activities. The activities determined for short time observations (0.4 second to 42 seconds after fission) are listed in Table 3 and the activities for the long time observations (0.7 minute to 152 minutes after fission) are listed in Table 4.

The sixteen full-energy (0-1130 keV) time-dependent spectra are displayed graphically in Figs. 7, 8, 9, and 10. The spectra were integrated over the counting intervals listed in Table 1 representing the mean times that are indicated on the figures. The data are normalized to a one-minute counting period, a one-sample observation, and a one-second irradiation time. The highest energy increment data were taken with a wider energy range than the other data resulting in a larger energy per channel factor. This accounts for the fact that there are fewer points in a peak at higher energies than at lower energies for the different spacings evident in the spectra.

TABLE 3
GAMMA ACTIVITY FOR EACH ANALYZER SUBGROUP, SHORT TIMES

| Gamma Energy (keV) | $\times 10^6$ dpm/sample - second irradiation | | | | | | | | Approximate Half-life |
|-----------------------|---|------------------|-----------------|-----------------|----------------|----------------|----------------|---------------|--------------------------|
| | 1 | 2 | 3 | 4 | 5 | 6 | 7 | 8 | |
| 67.27 \pm 0.42 | --- | --- | --- | --- | --- | 16. \pm 2. | 13. \pm 2. | 9.8 \pm 1.0 | --- |
| 78.77 \pm 0.57 | --- | --- | --- | 47. \pm 7. | 36. \pm 6. | 33. \pm 4. | 14. \pm 3. | 7.7 \pm 1.6 | 11. s \pm 3 s |
| 83.47 \pm 1.30 | --- | --- | --- | --- | 18. \pm 7. | 3.1 \pm 4.4 | 17. \pm 4. | 12. \pm 2. | --- |
| 92.55 \pm 0.35 | --- | 910. \pm 190. | 610. \pm 80. | 510. \pm 100. | 300. \pm 16. | 200. \pm 10. | 120. \pm 20. | 76. \pm 4. | --- |
| 96.38 \pm 0.32 | 1600. \pm 100. | 1500. \pm 220. | 1500. \pm 70. | 1100. \pm 90. | 590. \pm 18. | 420. \pm 11. | 250. \pm 23. | 130. \pm 4. | --- |
| 101.08 \pm 0.42 | 600. \pm 100. | 770. \pm 180. | 570. \pm 56. | 440. \pm 43. | 190. \pm 12. | 120. \pm 7. | 57. \pm 13. | 24. \pm 3. | --- |
| 108.43 \pm 0.38 | --- | --- | 920. \pm 52. | 720. \pm 47. | 300. \pm 23. | 170. \pm 27. | 100. \pm 81. | 57. \pm 4. | --- |
| 111.07 \pm 0.62 | 720. \pm 150. | 1200. \pm 220. | --- | --- | 200. \pm 23. | 170. \pm 27. | 88. \pm 76. | 27. \pm 5. | 9.5 s \pm 1.0 s |
| 114.97 \pm 0.89 | --- | --- | 560. \pm 58. | 330. \pm 53. | 110. \pm 16. | 78. \pm 11. | 34. \pm 41. | --- | 2.0 s \pm 0.2 s |
| 120.60 \pm 0.32 | 1700. \pm 170. | 1800. \pm 250. | 1500. \pm 54. | 860. \pm 44. | 240. \pm 19. | 120. \pm 83. | 73. \pm 16. | 56. \pm 3. | 30. s |
| 129.48 \pm 1.08 | --- | --- | 180. \pm 48. | 83. \pm 36. | 27. \pm 10. | 19. \pm 8. | 14. \pm 5. | 8.9 \pm 2.2 | 26. s \pm 13. s |
| 137.00 \pm 0.50 | 280. \pm 22. | 420. \pm 280. | 180. \pm 86. | 400. \pm 46. | 260. \pm 15. | 270. \pm 12. | 220. \pm 8. | 110. \pm 3. | --- |
| 141.99 \pm 0.75 | 170. \pm 210. | 580. \pm 280. | 650. \pm 90. | 350. \pm 46. | 160. \pm 14. | 71. \pm 10. | --- | --- | 1.8 s |
| 146.04 \pm 0.66 | --- | --- | --- | --- | 58. \pm 12. | --- | 20. \pm 5. | 11. \pm 3. | 13.0 s \pm 1.7 s |
| 156.59 \pm 0.64 | 710. \pm 130. | 740. \pm 300. | 270. \pm 65. | 320. \pm 110. | 230. \pm 21. | 110. \pm 24. | 81. \pm 21. | 25. \pm 9. | --- |
| 160.73 \pm 0.51 | 1300. \pm 140. | 1200. \pm 300. | 1300. \pm 80. | 640. \pm 100. | 350. \pm 20. | 170. \pm 23. | 50. \pm 21. | 13. \pm 3. | --- |
| 166.90 \pm 1.03 | 390. \pm 110. | 280. \pm 100. | 230. \pm 70. | --- | 51. \pm 14. | 33. \pm 12. | --- | 12. \pm 3. | --- |
| 174.10 \pm 0.50 | --- | --- | --- | 200. \pm 40. | 170. \pm 40. | 140. \pm 18. | 92. \pm 8. | 63. \pm 4. | 20. s \pm 3 s |
| 180.69 \pm 1.23 | --- | --- | --- | --- | 140. \pm 40. | 91. \pm 17. | 28. \pm 14. | 14. \pm 3. | 9. s \pm 2 s |
| 192.38 \pm 0.50 | --- | --- | --- | --- | --- | --- | --- | 18. \pm 3. | 16. m |
| 196.94 \pm 0.61 | 640. \pm 20. | 670. \pm 170. | 620. \pm 110. | 370. \pm 70. | 290. \pm 40. | 160. \pm 20. | 62. \pm 9. | 55. \pm 3. | --- |

TABLE 3 (Continued)

| Gamma Energy (keV) | $\times 10^6$ dpm/sample - second irradiation | | | | | | | | Approximate Half-life |
|-----------------------|---|------------------|------------------|-----------------|-----------------|----------------|-----------------|---------------|--------------------------------|
| | 1 | 2 | 3 | 4 | 5 | 6 | 7 | 8 | |
| 212.25 \pm 0.58 | 880. \pm 180. | 920. \pm 200. | 540. \pm 110 | 670. \pm 70. | 370. \pm 40. | 310. \pm 30. | 150. \pm 100. | 74. \pm 3. | 10. s \pm 4 s |
| 219.53 \pm 0.63 | 330. \pm 180. | 360. \pm 180. | 220. \pm 100. | 410. \pm 60. | 280. \pm 40. | 260. \pm 30. | 160. \pm 100. | 130. \pm 3. | 24. s \pm 10 s |
| 243.07 \pm 0.91 | --- | 820. \pm 180. | 230. \pm 140. | 370. \pm 70. | 170. \pm 50. | 120. \pm 30. | 53. \pm 8. | 35. \pm 6. | 26. s \pm 13 s |
| 253.14 \pm 1.23 | --- | 520. \pm 200. | 360. \pm 150. | 410. \pm 70. | 110. \pm 50. | --- | --- | --- | 1.8 s \pm 1 s |
| 259.63 \pm 0.67 | --- | 1000. \pm 230. | 730. \pm 180. | 670. \pm 90. | 430. \pm 60. | 390. \pm 40. | 220. \pm 10. | 70. \pm 7. | 9. s \pm 2 s |
| 269.70 \pm 0.60 | 750. \pm 260. | 440. \pm 170. | 250. \pm 80. | 110. \pm 40. | --- | 54. \pm 19. | 38. \pm 9. | 22. \pm 5. | 0.7 s, 20 s (2) |
| 276.24 \pm 0.34 | 1100. \pm 270. | --- | --- | 470. \pm 250. | 370. \pm 80. | 330. \pm 20. | 160. \pm 10. | 34. \pm 5. | 8. s \pm 1 s |
| 290.58 \pm 0.47 | --- | 620. \pm 340. | 210. \pm 110. | 410. \pm 50. | 320. \pm 60. | 220. \pm 20. | 120. \pm 60. | 74. \pm 6. | 14 s |
| 295.83 \pm 0.18 | 2700. \pm 350. | 3000. \pm 360. | 2500. \pm 260. | 1900. \pm 60. | 1200. \pm 80. | 640. \pm 30. | 180. \pm 20. | 76. \pm 6. | --- |
| 304.17 \pm 0.63 | 720. \pm 300 | 740. \pm 190. | 230. \pm 90. | 230. \pm 40. | --- | --- | --- | --- | 1 s \pm 0.7 s |
| 317.74 \pm 1.09 | --- | --- | --- | --- | --- | --- | --- | 11. \pm 6. | --- |
| 332.25 \pm 0.49 | --- | --- | --- | --- | --- | 96. \pm 21. | 43. \pm 7. | 30. \pm 7. | 15. s \pm 3 s |
| 336.80 \pm 0.94 | --- | --- | --- | --- | --- | 74. \pm 21. | 23. \pm 7. | 15. \pm 7. | 10. s \pm 5 s |
| 344.33 \pm 0.35 | --- | --- | --- | --- | --- | 91. \pm 19. | 82. \pm 8. | 63. \pm 9. | 48. s \pm 13 s |
| 351.20 \pm 0.49 | 1200. \pm 310. | 1100. \pm 180. | 420. \pm 100. | --- | --- | --- | --- | --- | 0.3 s \pm 0.1 s ^a |
| 354.87 \pm 0.70 | --- | --- | --- | 310. \pm 100. | 160. \pm 80. | 90. \pm 23. | 30. \pm 8. | 28. \pm 7. | 4. s \pm 3 s |
| 359.10 \pm 0.43 | --- | 1500. \pm 190. | 1100. \pm 120. | 740. \pm 100. | 400. \pm 90. | 110. \pm 30. | --- | --- | 1.5 s \pm 0.2 s |
| 362.75 \pm 0.60 | --- | --- | --- | --- | --- | 87. \pm 35. | 40. \pm 8. | 30. \pm 7. | 20. s \pm 9 s |
| 368.13 \pm 0.54 | --- | --- | --- | --- | --- | --- | --- | 27. \pm 7. | --- |
| 375.68 \pm 0.83 | 820. \pm 320. | 860. \pm 190. | 240. \pm 110. | --- | --- | --- | --- | --- | --- |
| 380.56 \pm 0.54 | --- | --- | --- | 83. \pm 91. | 250. \pm 90. | 120. \pm 30. | 120. \pm 10. | 97. \pm 8. | --- |

^a Precursor: 0.1 s

TABLE 3 (Continued)

| Gamma Energy (keV) | $\times 10^6$ dpm/sample - second irradiation | | | | | | | | Approximate Half-life |
|-----------------------|---|------------------|-------------------|------------------|------------------|-----------------|----------------|----------------|------------------------------|
| | 1 | 2 | 3 | 4 | 5 | 6 | 7 | 8 | |
| 387.09 \pm 0.56 | 660. \pm 310. | 580. \pm 180. | 700. \pm 120. | 360. \pm 160. | 380. \pm 110. | 160. \pm 30. | 95. \pm 12. | 44. \pm 7. | 6. s \pm 2 s |
| 396.67 \pm 0.42 | --- | --- | --- | --- | 290. \pm 180. | 180. \pm 70. | 220. \pm 30. | 250. \pm 10. | 45. s \pm 3 s ^b |
| 399.89 \pm 0.46 | 1200. \pm 30. | 630. \pm 180. | 1100. \pm 120. | 720. \pm 100. | 460. \pm 180. | 250. \pm 70. | 150. \pm 25. | 55. \pm 11. | 4. s \pm 2 s |
| 406.02 \pm 0.92 | --- | 660. \pm 200. | 320. \pm 180. | 320. \pm 110. | --- | --- | --- | --- | |
| 408.71 \pm 0.52 | --- | --- | --- | 440. \pm 110. | 320. \pm 60. | 100. \pm 50. | 140. \pm 8. | 51. \pm 7. | 10. s \pm 1 s |
| 413.00 \pm 0.76 | 760. \pm 340. | 690. \pm 200. | --- | --- | 190. \pm 60. | --- | --- | --- | 1.6 s \pm 0.6 s |
| 430.36 \pm 0.61 | --- | 910. \pm 300. | 810. \pm 240. | 370. \pm 150. | 460. \pm 80. | 300. \pm 150. | 250. \pm 30. | 69. \pm 17. | 7.5 s \pm 2 s |
| 432.72 \pm 0.82 | --- | --- | --- | 670. \pm 150. | --- | 190. \pm 150. | --- | 44. \pm 16. | 7.5 s \pm 2 s |
| 461.19 \pm 0.70 | --- | 600. \pm 270. | 880. \pm 230. | 530. \pm 130. | 280. \pm 70. | 160. \pm 40. | --- | --- | 2.5 s \pm 0.7 s |
| 466.24 \pm 0.87 | --- | --- | 1500. \pm 1200. | 660. \pm 340. | 1000. \pm 390. | 130. \pm 80. | 77. \pm 25. | 32. \pm 7. | --- |
| 469.46 \pm 0.49 | 4300. \pm 580. | 3700. \pm 370. | 2500. \pm 1200. | 550. \pm 390. | 550. \pm 390. | 470. \pm 90. | 69. \pm 25. | --- | 2.2 s \pm 0.4 s |
| 482.86 \pm 0.91 | --- | --- | --- | --- | --- | 90. \pm 31. | 45. \pm 19. | 17. \pm 7. | 10. s \pm 3 s |
| 503.68 \pm 0.34 | 1700. \pm 390. | 1200. \pm 250. | 1500. \pm 390. | 1000. \pm 130. | 640. \pm 20. | 620. \pm 30. | 260. \pm 20. | 78. \pm 8. | 7. s \pm 2 s |
| 509.08 \pm 0.81 | 1200. \pm 360. | 630. \pm 240. | 560. \pm 360. | 470. \pm 120. | 190. \pm 15. | --- | --- | --- | 1.4 s \pm 0.4 s |
| 509.88 \pm 0.69 | --- | --- | --- | --- | 170. \pm 50. | 160. \pm 30. | 94. \pm 18. | 40. \pm 11. | 13. s \pm 7 s |
| 513.27 \pm 0.49 | --- | --- | 600. \pm 250. | --- | --- | 230. \pm 30. | 99. \pm 14. | 42. \pm 7. | 7. s \pm 2 s |
| 528.16 \pm 0.51 | --- | --- | 820. \pm 170. | 520. \pm 110. | 90. \pm 41. | 290. \pm 40. | 110. \pm 10. | 32. \pm 9. | 6. s \pm 3 s |
| 533.78 \pm 0.26 | 2600. \pm 470. | 2400. \pm 340. | 2200. \pm 300. | 2300. \pm 160. | 1300. \pm 170. | 1100. \pm 50. | 470. \pm 30. | 110. \pm 10. | 6.5 s \pm 1.0 s |
| 538.98 \pm 0.54 | 820. \pm 410. | 1200. \pm 310. | 1200. \pm 290. | 1200. \pm 250. | 360. \pm 150. | 390. \pm 40. | 310. \pm 30. | 230. \pm 10. | 45. s \pm 3 s |
| 544.64 \pm 0.25 | 5200. \pm 520. | 3900. \pm 340. | 3700. \pm 290. | 2200. \pm 280. | 1300. \pm 110. | 510. \pm 50. | --- | --- | 2. s \pm 0.3 s |
| 552.72 \pm 0.67 | --- | --- | --- | --- | --- | 170. \pm 30. | 70. \pm 17. | 24. \pm 7. | 8.7 s \pm 1.7 s |

^b Precursor: 7 s

TABLE 3 (Continued)

| Gamma Energy (keV) | $\times 10^6$ dpm/sample - second irradiation | | | | | | | | Approximate Half-life |
|-----------------------|---|------------------|------------------|------------------|-----------------|----------------|----------------|---------------|--------------------------|
| | 1 | 2 | 3 | 4 | 5 | 6 | 7 | 8 | |
| 568.89 \pm 1.56 | --- | --- | --- | --- | 150. \pm 80. | 60. \pm 36. | 41. \pm 18. | 8. \pm 7. | 7.5 s \pm 1.5 s |
| 570.75 \pm 1.14 | --- | 610. \pm 340. | 670. \pm 230. | --- | --- | --- | --- | --- | --- |
| 576.04 \pm 0.54 | --- | --- | --- | --- | --- | --- | 70. \pm 17. | 37. \pm 6. | 17. s \pm 6 s |
| 583.95 \pm 0.57 | --- | --- | --- | --- | --- | --- | 84. \pm 26. | 59. \pm 10. | 32. s \pm 17 s |
| 585.55 \pm 0.76 | 1600. \pm 530. | 1500. \pm 380. | --- | --- | --- | --- | --- | --- | 3. s \pm 2 s |
| 587.81 \pm 0.60 | --- | --- | 910. \pm 320. | 930. \pm 170. | --- | --- | 150. \pm 30. | 61. \pm 10. | 8. s |
| 592.06 \pm 0.59 | 2200. \pm 540. | 2300. \pm 410. | 1300. \pm 340. | 1100. \pm 170. | 740. \pm 110. | 190. \pm 40. | --- | --- | 1.7 s \pm 0.2 s |
| 596.40 \pm 0.89 | --- | --- | 1300. \pm 400. | --- | --- | 140. \pm 40. | 85. \pm 27. | --- | --- |
| 600.68 \pm 0.33 | --- | --- | 850. \pm 190. | 940. \pm 110. | 540. \pm 70. | 340. \pm 40. | 210. \pm 30. | 190. \pm 9. | 1.02m \pm 0.1 m |
| 610.30 \pm 0.77 | 1600. \pm 520. | 1100. \pm 380. | 810. \pm 190. | 390. \pm 110. | 290. \pm 70. | 90. \pm 40. | 87. \pm 18. | 31. \pm 8. | 1.7 s \pm 0.7 s |
| 616.75 \pm 0.68 | --- | --- | 950. \pm 190. | 420. \pm 100. | 270. \pm 70. | 130. \pm 40. | 70. \pm 18. | 43. \pm 8. | --- |
| 639.38 \pm 0.72 | --- | --- | 550. \pm 190. | 510. \pm 110. | --- | --- | --- | --- | 9. s \pm 5 s |
| 643.24 \pm 0.97 | --- | --- | --- | --- | 200. \pm 70. | 140. \pm 30. | 46. \pm 19. | 25. \pm 12. | 7. s \pm 3 s |
| 683.76 \pm 0.81 | 1500. \pm 600. | 800. \pm 420. | --- | 260. \pm 110. | 150. \pm 70. | 250. \pm 40. | 120. \pm 20. | 91. \pm 16. | --- |
| 706.45 \pm 0.70 | --- | --- | --- | 450. \pm 120. | 310. \pm 80. | 200. \pm 40. | --- | --- | 4. s \pm 0.2 s |
| 709.62 \pm 0.75 | --- | --- | --- | --- | --- | --- | 87. \pm 23. | --- | --- |
| 720.71 \pm 0.88 | --- | --- | --- | --- | 270. \pm 80. | 130. \pm 40. | --- | --- | 3.2 s \pm 0.5 s |
| 724.72 \pm 0.76 | 2500. \pm 700. | --- | --- | --- | --- | --- | --- | --- | --- |
| 764.10 \pm 0.82 | --- | --- | --- | --- | --- | --- | 110. \pm 30. | 57. \pm 18. | 17. s \pm 8 s |
| 769.81 \pm 0.74 | --- | --- | --- | --- | --- | 300. \pm 50. | 160. \pm 30. | --- | 9. s \pm 4 s |

TABLE 3 (Continued)

| Gamma Energy (keV) | $\times 10^6$ dpm/sample - second irradiation | | | | | | | | Approximate Half-life |
|-----------------------|---|------------------|------------------|------------------|-----------------|----------------|----------------|----------------|--------------------------|
| | 1 | 2 | 3 | 4 | 5 | 6 | 7 | 8 | |
| 776.34 \pm 0.34 | --- | --- | --- | 570. \pm 140. | 520. \pm 110. | 350. \pm 40. | 230. \pm 20. | 120. \pm 10. | 13. s \pm 3 s |
| 788.29 \pm 0.38 | --- | --- | --- | --- | --- | --- | --- | 76. \pm 11. | 16. s \pm 3 s |
| 800.15 \pm 0.42 | --- | --- | --- | --- | 450. \pm 110. | 270. \pm 50. | 180. \pm 30. | 92. \pm 14. | 15. s \pm 2 s |
| 806.49 \pm 0.57 | --- | --- | --- | --- | --- | 250. \pm 50. | 130. \pm 20. | 55. \pm 13. | 11. s \pm 3 s |
| 809.83 \pm 0.22 | 6900. \pm 490. | 5800. \pm 480. | 4300. \pm 370. | 2200. \pm 190. | 950. \pm 130. | --- | --- | --- | 11. s \pm 1 s |
| 817.19 \pm 0.93 | 1200. \pm 350. | 780. \pm 330. | --- | --- | --- | --- | --- | --- | 5. s \pm 3 s |
| 837.09 \pm 0.40 | 2600. \pm 390. | 2400. \pm 390. | 1900. \pm 300. | 1200. \pm 170. | 740. \pm 130. | 340. \pm 50. | --- | --- | 19. s \pm 4 s |
| 846.15 \pm 0.70 | --- | --- | --- | 380. \pm 140. | 380. \pm 110. | 120. \pm 40. | 110. \pm 20. | 86. \pm 13. | 39. s \pm 7 s |
| 875.28 \pm 0.89 | --- | --- | --- | --- | 360. \pm 130. | 160. \pm 50. | 72. \pm 26. | --- | 4. s \pm 3 s |
| 896.69 \pm 0.84 | --- | --- | --- | --- | --- | 160. \pm 60. | 70. \pm 19. | 52. \pm 14. | 18. s \pm 10 s |
| 913.90 \pm 0.74 | --- | --- | --- | 640. \pm 170. | 310. \pm 100. | 140. \pm 60. | 93. \pm 20. | 63. \pm 14. | --- |
| 928.24 \pm 0.90 | --- | --- | --- | 480. \pm 170. | 440. \pm 110. | 140. \pm 60. | 55. \pm 20. | --- | 3.7s \pm 0.6s |
| 933.31 \pm 1.09 | 1700. \pm 790. | 990. \pm 410. | 920. \pm 310. | --- | --- | --- | --- | --- | 0.7s |
| 969.26 \pm 0.63 | 4000. \pm 980. | 2800. \pm 520. | 2300. \pm 360. | 1300. \pm 180. | 600. \pm 130. | 220. \pm 70. | 85. \pm 23. | --- | --- |
| 974.29 \pm 0.82 | --- | --- | --- | --- | --- | --- | --- | 68. \pm 17. | 1.6m \pm 0.4m |
| 981.11 \pm 0.93 | --- | --- | --- | --- | 340. \pm 120. | 150. \pm 70. | 120. \pm 20. | 45. \pm 16. | 9 s \pm 3 s |
| 1003.29 \pm 1.06 | --- | 1400. \pm 490. | 1200. \pm 340. | 650. \pm 160. | --- | --- | --- | --- | 1.2s \pm 0.4s |
| 1011.01 \pm 1.01 | --- | --- | --- | --- | 310. \pm 120. | 160. \pm 70. | 84. \pm 24. | 42. \pm 17. | --- |
| 1023.33 \pm 0.90 | --- | --- | --- | --- | 420. \pm 130. | 240. \pm 70. | 120. \pm 20. | 34. \pm 16. | 8 s \pm 2 s |
| 1102.79 \pm 0.63 | 6600. \pm 150. | 6200. \pm 730. | 5200. \pm 570. | 1900. \pm 260. | 880. \pm 150. | 290. \pm 80. | --- | --- | 1.1s |

TABLE 3 (Continued)

| Gamma Energy (keV) | $\times 10^6$ dpm/sample - second irradiation | | | | | | | | Approximate Half-life |
|-----------------------|---|-----------------|------------------|-----------------|-----------------|----------------|----------------|----------------|--------------------------|
| | 1 | 2 | 3 | 4 | 5 | 6 | 7 | 8 | |
| 1107.82 \pm 1.02 | 2200. \pm 130. | --- | 1300. \pm 430. | 510. \pm 220. | 450. \pm 130. | 330. \pm 80. | 190. \pm 40. | 74. \pm 24. | 11. s |
| 1118.33 \pm 0.80 | --- | --- | 1000. \pm 370. | 560. \pm 170. | 470. \pm 120. | 280. \pm 80. | 300. \pm 40. | 260. \pm 30. | 47. s \pm 7 s |
| 1127.38 \pm 1.65 | 1100. \pm 900. | 670. \pm 490. | 630. \pm 350. | 230. \pm 160. | 190. \pm 110. | --- | 110. \pm 40. | 68. \pm 28. | 17. s |

TABLE 4

GAMMA ACTIVITY FOR EACH ANALYZER SUBGROUP, LONG TIMES

| Gamma Energy (keV) | $\times 10^4$ dpm/sample - second irradiation | | | | | | | | Approximate Half-life |
|-----------------------|---|------------------|-----------------|----------------|----------------|----------------|---------------|---------------|--------------------------|
| | 1 | 2 | 3 | 4 | 5 | 6 | 7 | 8 | |
| 67.27 \pm 0.46 | 330. \pm 40. | 200. \pm 30. | 71. \pm 12. | 15. \pm 4. | 10. \pm 4. | --- | 2. \pm 0.6 | 1.3 \pm 0.4 | --- |
| 72.29 \pm 0.44 | --- | --- | --- | --- | 18. \pm 5. | --- | 5.1 \pm 0.8 | 2.5 \pm 0.5 | 36 m |
| 76.30 \pm 0.27 | --- | --- | 120. \pm 20. | 58. \pm 6. | 61. \pm 7. | --- | 18. \pm 1. | 7. \pm 0.6 | 32 m |
| 82.01 \pm 0.60 | 220. \pm 70. | 190. \pm 50. | --- | --- | --- | --- | --- | --- | --- |
| 92.54 \pm 0.22 | 2800. \pm 200. | 1700. \pm 90. | 640. \pm 20. | 220. \pm 20. | 160. \pm 10. | 74. \pm 4. | 32. \pm 3. | 14. \pm 1. | --- |
| 96.60 \pm 0.23 | 4700. \pm 260. | 2000. \pm 100. | 870. \pm 30. | 410. \pm 30. | 180. \pm 20. | 120. \pm 5. | 57. \pm 3. | 22. \pm 1. | --- |
| 102.33 \pm 0.56 | 390. \pm 150. | 230. \pm 60. | 99. \pm 17. | 67. \pm 17. | 32. \pm 9. | --- | --- | --- | --- |
| 109.62 \pm 0.34 | 1500. \pm 190. | 790. \pm 80. | 340. \pm 20. | 210. \pm 20. | 110. \pm 15. | 56. \pm 4. | 20. \pm 3. | 10. \pm 1. | --- |
| 113.32 \pm 0.60 | --- | --- | 50. \pm 20. | 57. \pm 20. | 61. \pm 14. | 18. \pm 4. | 14. \pm 4. | 6.8 \pm 1.5 | --- |
| 120.69 \pm 0.38 | 2100. \pm 220. | 870. \pm 90. | 64. \pm 22. | --- | --- | --- | --- | --- | 30 s |
| 136.32 \pm 0.47 | 1800. \pm 240. | 580. \pm 120. | 210. \pm 30. | 83. \pm 21. | --- | --- | --- | --- | --- |
| 138.11 \pm 0.50 | --- | --- | --- | --- | --- | --- | 13. \pm 3. | 8.6 \pm 1.5 | 96 m \pm 48 m |
| 149.44 \pm 0.42 | --- | --- | --- | 150. \pm 30. | 92. \pm 16. | 72. \pm 8. | 71. \pm 5. | 28. \pm 2. | 51 m |
| 153.79 \pm 0.82 | --- | --- | --- | 53. \pm 23. | 40. \pm 14. | 25. \pm 7. | --- | --- | 22 m \pm 10 m |
| 166.01 \pm 0.46 | --- | --- | --- | --- | --- | --- | 43. \pm 5. | 21. \pm 4. | 57 m \pm 21 m |
| 167.90 \pm 0.59 | --- | --- | 370. \pm 50. | 190. \pm 30. | 110. \pm 20. | 57. \pm 7. | --- | 5.4 \pm 3.1 | --- |
| 175.10 \pm 0.61 | 2200. \pm 360. | 930. \pm 180. | 270. \pm 40. | 57. \pm 30. | --- | --- | --- | --- | 1 m |
| 181.78 \pm 0.55 | --- | --- | 200. \pm 40. | 150. \pm 30. | 150. \pm 20. | 81. \pm 10. | 47. \pm 6. | 18. \pm 3. | 30 m |
| 191.26 \pm 0.51 | --- | 1000. \pm 220. | 930. \pm 100. | 580. \pm 50. | 430. \pm 30. | 210. \pm 10. | 76. \pm 7. | 11. \pm 3. | 16 m |
| 197.07 \pm 0.71 | 2700. \pm 430. | 1100. \pm 220. | 320. \pm 80. | 89. \pm 32. | 42. \pm 22. | --- | --- | --- | --- |

TABLE 4 (Continued)

| Gamma Energy (keV) | $\times 10^4$ dpm/sample - second irradiation | | | | | | | | Approximate Half-life |
|-----------------------|---|------------------|------------------|----------------|----------------|----------------|----------------|---------------|------------------------------|
| | 1 | 2 | 3 | 4 | 5 | 6 | 7 | 8 | |
| 211.46 \pm 0.66 | 1600. \pm 450. | 550. \pm 220. | 350. \pm 90. | 170. \pm 40. | 120. \pm 20. | 96. \pm 16. | 62. \pm 8. | 28. \pm 4. | --- |
| 219.84 \pm 0.60 | 6900. \pm 670. | 2900. \pm 340. | 960. \pm 110. | 240. \pm 40. | 81. \pm 24. | --- | --- | --- | --- |
| 231.72 \pm 0.86 | --- | --- | 280. \pm 100. | 140. \pm 40. | 79. \pm 26. | --- | --- | --- | 7 m \pm 4 m |
| 255.32 \pm 0.87 | --- | --- | --- | 160. \pm 50. | 140. \pm 40. | 120. \pm 40. | --- | --- | 66 m |
| 259.01 \pm 0.71 | --- | --- | 740. \pm 130. | 590. \pm 60. | 390. \pm 50. | 130. \pm 40. | 57. \pm 10. | --- | 13 m \pm 4 m |
| 270.36 \pm 0.82 | --- | 930. \pm 130. | 340. \pm 90. | 100. \pm 20. | 25. \pm 15. | --- | 12. \pm 5. | 3.8 \pm 1.6 | 2 m \pm 1 m |
| 276.95 \pm 0.27 | 710. \pm 390. | 410. \pm 120. | 500. \pm 90. | 400. \pm 30. | 290. \pm 20. | 190. \pm 20. | 90. \pm 7. | 24. \pm 2. | 23 m \pm 3 m |
| 283.92 \pm 0.67 | --- | 360. \pm 130. | 280. \pm 100. | 160. \pm 20. | --- | --- | --- | --- | 4.5m \pm 1.5m |
| 289.30 \pm 0.47 | 2700. \pm 280. | 920. \pm 140. | 340. \pm 100. | --- | --- | --- | --- | --- | 77 s \pm 30 s |
| 292.84 \pm 0.56 | --- | --- | --- | --- | --- | --- | 14. \pm 5. | 10. \pm 2. | 2 hr \pm 1.3hr |
| 295.94 \pm 0.41 | 3300. \pm 330. | 1100. \pm 150. | 290. \pm 100. | --- | --- | --- | --- | --- | --- |
| 301.83 \pm 0.34 | 1600. \pm 290. | 950. \pm 140. | 1100. \pm 130. | 480. \pm 40. | 200. \pm 50. | --- | --- | --- | 4.5m \pm 1 m |
| 305.66 \pm 0.18 | --- | --- | --- | 460. \pm 40. | 460. \pm 50. | 510. \pm 30. | 250. \pm 10. | 43. \pm 2. | 23.5m \pm 1 m ^a |
| 311.11 \pm 0.36 | --- | --- | 430. \pm 80. | 470. \pm 40. | 360. \pm 30. | 180. \pm 20. | 57. \pm 9. | 11. \pm 2. | 15 m \pm 2 m |
| 315.53 \pm 0.46 | --- | --- | 340. \pm 80. | 360. \pm 30. | 200. \pm 20. | 130. \pm 20. | 29. \pm 9. | 4.5 \pm 1.7 | 16 m \pm 2 m |
| 329.53 \pm 1.00 | --- | --- | --- | --- | 37. \pm 27. | 33. \pm 18. | --- | 10. \pm 2. | 51 m \pm 17 m |
| 334.26 \pm 0.74 | --- | --- | --- | --- | 73. \pm 27. | 42. \pm 18. | --- | 9.6 \pm 1.9 | 34 m \pm 15 m |
| 342.87 \pm 0.54 | --- | --- | 340. \pm 430. | 260. \pm 40. | 130. \pm 10. | 67. \pm 9. | 22. \pm 5. | --- | 13 m \pm 3 m |
| 345.60 \pm 1.37 | --- | --- | 430. \pm 430. | --- | --- | --- | --- | --- | 48 s \pm 13 s ^b |

^a Precursor: 7.5 m^b Determination made from matching energy in Table 3

TABLE 4 (Continued)

| Gamma Energy (keV) | $\times 10^4$ dpm/sample - second irradiation | | | | | | | | Approximate Half-life |
|-----------------------|---|------------------|------------------|----------------|----------------|----------------|----------------|--------------|-----------------------------|
| | 1 | 2 | 3 | 4 | 5 | 6 | 7 | 8 | |
| 348.63 \pm 0.47 | --- | --- | --- | 170. \pm 40. | 70. \pm 10. | --- | --- | --- | 6 m \pm 2 m |
| 356.57 \pm 0.27 | --- | --- | 250. \pm 80. | 280. \pm 40. | 200. \pm 10. | 120. \pm 10. | 50. \pm 5. | --- | 20 m \pm 2 m |
| 380.91 \pm 0.40 | 5000. \pm 610. | 1500. \pm 270. | 530. \pm 80. | 130. \pm 30. | --- | --- | --- | --- | --- |
| 396.42 \pm 0.18 | 13000. \pm 800. | 6300. \pm 390. | 1200. \pm 90. | 200. \pm 30. | --- | --- | --- | --- | 45 s \pm 3 s ^c |
| 402.08 \pm 0.42 | --- | --- | --- | 230. \pm 40. | 110. \pm 20. | 55. \pm 12. | 68. \pm 7. | 40. \pm 4. | 72 m \pm 11 m |
| 407.10 \pm 0.34 | 1900. \pm 530. | 1400. \pm 280. | 1200. \pm 100. | 580. \pm 50. | 300. \pm 30. | 120. \pm 10. | 51. \pm 7. | 22. \pm 3. | --- |
| 423.37 \pm 0.64 | --- | --- | 440. \pm 90. | 160. \pm 40. | 94. \pm 36. | --- | --- | --- | 4 m \pm 3 m |
| 434.15 \pm 0.30 | --- | 1000. \pm 270. | 670. \pm 100. | 480. \pm 50. | 390. \pm 30. | 230. \pm 20. | 94. \pm 8. | 33. \pm 4. | 28 m \pm 3 m |
| 452.95 \pm 0.40 | --- | --- | --- | --- | 150. \pm 40. | 140. \pm 30. | 120. \pm 10. | 34. \pm 4. | 34 m \pm 5 m ^d |
| 455.42 \pm 0.43 | --- | 1900. \pm 340. | 1300. \pm 130. | 810. \pm 60. | 250. \pm 40. | 56. \pm 24. | 45. \pm 9. | --- | 4.4 m \pm 0.4 m |
| 462.44 \pm 0.32 | --- | --- | 260. \pm 90. | 260. \pm 50. | 250. \pm 30. | 240. \pm 20. | 140. \pm 10. | 61. \pm 5. | 50 m \pm 8 m |
| 488.10 \pm 0.57 | --- | --- | --- | --- | --- | --- | --- | 13. \pm 3. | --- |
| 506.94 \pm 0.60 | --- | --- | --- | --- | 110. \pm 30. | 66. \pm 15. | --- | --- | 19 m \pm 8 m |
| 509.47 \pm 0.63 | --- | --- | --- | --- | --- | 100. \pm 20. | 33. \pm 10. | 13. \pm 4. | 25 m \pm 11 m |
| 510.43 \pm 0.47 | --- | --- | --- | --- | --- | --- | 26. \pm 6. | 21. \pm 3. | annihilation |
| 513.03 \pm 0.79 | --- | --- | --- | --- | --- | --- | 29. \pm 10. | 17. \pm 5. | 76 m \pm 40 m |
| 529.69 \pm 0.52 | --- | --- | --- | --- | 120. \pm 30. | 79. \pm 17. | 42. \pm 8. | 26. \pm 6. | 28 m \pm 22 m |
| 539.81 \pm 0.18 | 11000. \pm 600. | 4700. \pm 270. | 920. \pm 120. | --- | --- | --- | --- | --- | 45 s \pm 3 s |
| 545.56 \pm 0.34 | --- | --- | --- | --- | --- | 120. \pm 20. | 88. \pm 9. | --- | 66 m \pm 34 m |

^c Precursor: 7 s^d Precursor: 8 m

TABLE 4 (Continued)

| Gamma Energy (keV) | $\times 10^4$ dpm/sample - second irradiation | | | | | | | | Approximate Half-life |
|-----------------------|---|------------------|------------------|------------------|----------------|----------------|----------------|----------------|-----------------------------|
| | 1 | 2 | 3 | 4 | 5 | 6 | 7 | 8 | |
| 565.63 \pm 0.53 | --- | --- | --- | 220. \pm 60. | 130. \pm 40. | 85. \pm 18. | 62. \pm 9. | 23. \pm 6. | 38 m \pm 15 m |
| 585.27 \pm 0.51 | 3300. \pm 620. | 1800. \pm 280. | 850. \pm 190. | 580. \pm 120. | --- | --- | --- | --- | --- |
| 589.92 \pm 0.32 | 3000. \pm 610. | 2700. \pm 300. | 2100. \pm 220. | 1600. \pm 140. | 900. \pm 60. | 280. \pm 30. | 41. \pm 9. | --- | 8.5m \pm 0.5m |
| 594.95 \pm 0.72 | --- | --- | --- | --- | --- | --- | 26. \pm 9. | 26. \pm 7. | --- |
| 601.93 \pm 0.23 | 9900. \pm 680. | 5100. \pm 330. | 1600. \pm 160. | --- | --- | --- | --- | --- | 1.02m \pm 0.1m |
| 621.32 \pm 0.60 | --- | --- | --- | --- | --- | 74. \pm 22. | 45. \pm 10. | 32. \pm 7. | 62 m \pm 19 m |
| 641.32 \pm 0.30 | --- | --- | --- | --- | 340. \pm 50. | 300. \pm 30. | 170. \pm 20. | 100. \pm 10. | 56 m \pm 7 m |
| 657.11 \pm 0.60 | --- | --- | --- | --- | 180. \pm 40. | 120. \pm 30. | 42. \pm 11. | 38. \pm 8. | 21 m \pm 4 m |
| 697.05 \pm 0.46 | --- | 2600. \pm 350. | 2100. \pm 220. | 960. \pm 120. | 290. \pm 50. | 76. \pm 26. | --- | --- | 18 m \pm 4 m |
| 710.56 \pm 0.63 | --- | 740. \pm 290. | 700. \pm 170. | 450. \pm 100. | 320. \pm 50. | 130. \pm 30. | --- | --- | 10.5m \pm 2 m |
| 724.11 \pm 0.43 | --- | 3100. \pm 360. | 2200. \pm 220. | 950. \pm 120. | 260. \pm 50. | --- | --- | --- | 17 m \pm 2 m |
| 743.06 \pm 0.58 | --- | --- | --- | 310. \pm 100. | 260. \pm 50. | 160. \pm 30. | 93. \pm 16. | 55. \pm 11. | 31 m \pm 8 m |
| 769.36 \pm 0.34 | --- | --- | 610. \pm 130. | 330. \pm 60. | 260. \pm 40. | 190. \pm 20. | 130. \pm 20. | 55. \pm 7. | --- |
| 776.66 \pm 0.57 | 2600. \pm 460. | --- | --- | --- | --- | --- | --- | --- | 13 s \pm 3 s ^e |
| 782.24 \pm 0.63 | 1900. \pm 450. | --- | 570. \pm 130. | 290. \pm 60. | --- | --- | --- | --- | 2.5m \pm 0.5m |
| 789.05 \pm 0.57 | 2100. \pm 450. | --- | --- | --- | --- | --- | --- | --- | 16 s \pm 3 s ^e |
| 795.05 \pm 0.48 | --- | --- | 620. \pm 130. | 470. \pm 60. | 370. \pm 40. | 120. \pm 20. | 42. \pm 12. | --- | 12 m \pm 1 m |
| 799.90 \pm 0.38 | 2800. \pm 450. | --- | --- | --- | --- | --- | --- | --- | 15 s \pm 2 s ^e |
| 804.57 \pm 0.93 | --- | --- | --- | --- | 84. \pm 38. | 60. \pm 16. | --- | --- | 34 m \pm 12 m |
| 817.26 \pm 0.71 | --- | 720. \pm 260. | 750. \pm 150. | 290. \pm 60. | 120. \pm 40. | 48. \pm 16. | --- | --- | 6 m |

^e Determination made from matching energy in Table 3

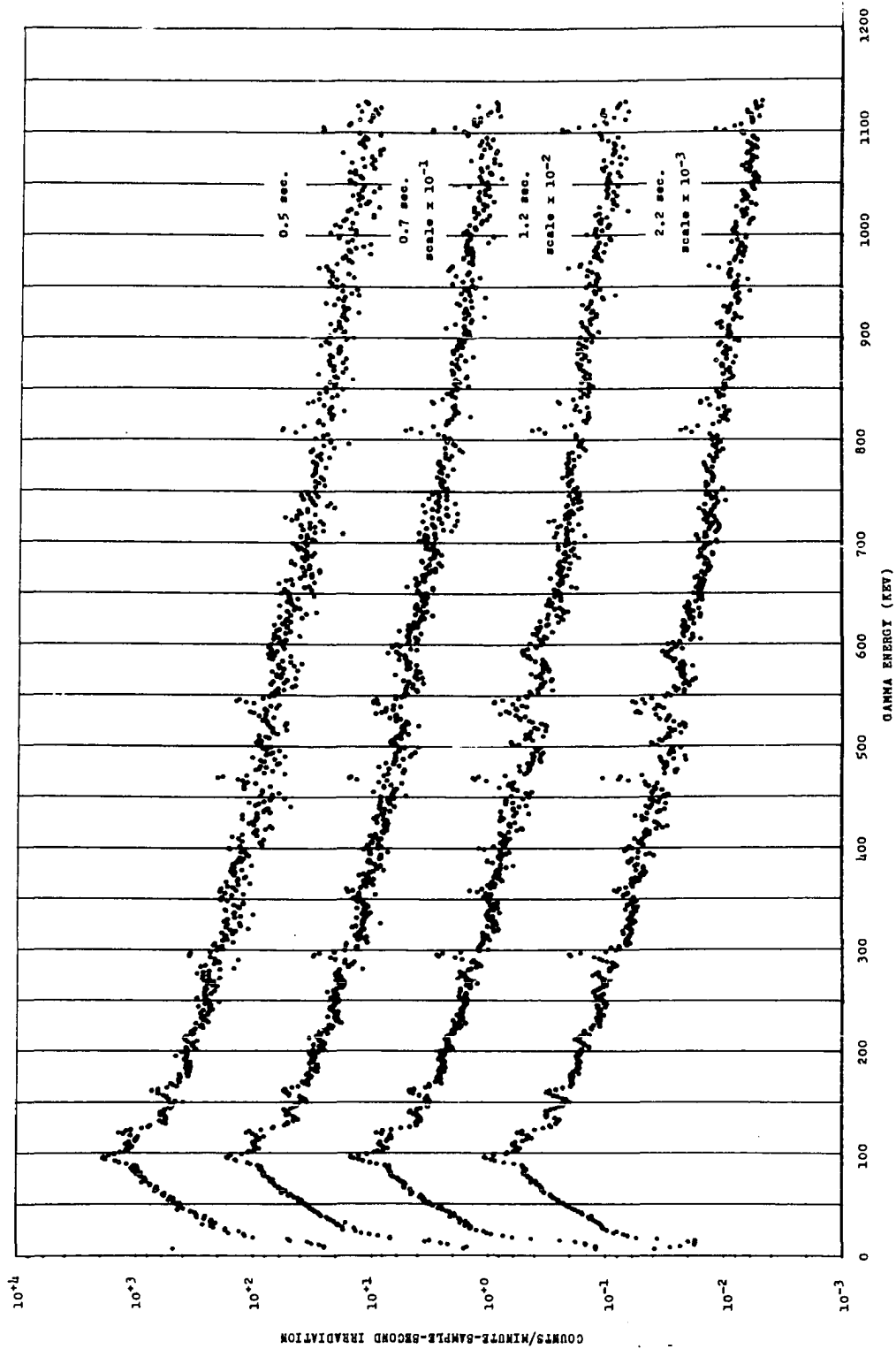
TABLE 4 (Continued)

| Gamma Energy (keV) | $\times 10^4$ dpm/sample - second irradiation | | | | | | | | Approximate Half-life |
|-----------------------|---|------------------|------------------|------------------|----------------|----------------|----------------|----------------|--------------------------------|
| | 1 | 2 | 3 | 4 | 5 | 6 | 7 | 8 | |
| 832.33 \pm 0.27 | 4000. \pm 500. | 3100. \pm 320. | 2400. \pm 190. | 1100. \pm 120. | 370. \pm 40. | --- | --- | --- | 4. m \pm 0.5m |
| 839.88 \pm 0.38 | --- | --- | 890. \pm 160. | 700. \pm 100. | 450. \pm 50. | 160. \pm 20. | --- | --- | 11. m \pm 1 m |
| 844.47 \pm 0.40 | 4300. \pm 540. | 1900. \pm 300. | 710. \pm 150. | --- | --- | --- | --- | --- | 39. s \pm 7 s |
| 847.39 \pm 0.31 | --- | --- | --- | 150. \pm 80. | 230. \pm 40. | 230. \pm 30. | 340. \pm 20. | 260. \pm 10. | --- |
| 876.57 \pm 0.49 | --- | --- | 720. \pm 180. | 630. \pm 110. | 340. \pm 50. | 110. \pm 20. | --- | --- | 9.1m \pm 1.5m |
| 884.31 \pm 0.34 | --- | --- | --- | --- | 200. \pm 50. | 290. \pm 30. | 260. \pm 20. | 180. \pm 10. | 106. m \pm 25 m ^f |
| 888.94 \pm 0.53 | --- | --- | 970. \pm 190. | 550. \pm 100. | 250. \pm 50. | --- | --- | --- | 6. m \pm 1.5m |
| 895.31 \pm 0.60 | --- | --- | --- | --- | 180. \pm 40. | 120. \pm 20. | 62. \pm 14. | --- | 26. m \pm 12 m |
| 913.13 \pm 0.44 | --- | --- | --- | --- | 230. \pm 40. | 190. \pm 30. | 130. \pm 20. | 63. \pm 9. | 54. m \pm 12 m |
| 918.95 \pm 0.41 | --- | --- | 850. \pm 200. | 730. \pm 120. | 600. \pm 50. | 400. \pm 40. | 150. \pm 20. | 32. \pm 8. | 23. m \pm 1 m |
| 933.52 \pm 0.78 | --- | --- | --- | --- | 170. \pm 30. | 92. \pm 28. | 43. \pm 17. | 15. \pm 6. | 22. m \pm 9 m |
| 943.56 \pm 1.39 | --- | --- | --- | 190. \pm 90. | 180. \pm 40. | 150. \pm 40. | 53. \pm 24. | 2.9 \pm 5.3 | 14. m |
| 948.32 \pm 1.26 | --- | --- | 540. \pm 200. | 280. \pm 120. | 250. \pm 40. | 120. \pm 40. | 47. \pm 23. | 13. \pm 7. | 17. m |
| 953.67 \pm 1.16 | --- | --- | 730. \pm 200. | 380. \pm 130. | 240. \pm 30. | 87. \pm 31. | 17. \pm 20. | 8.5 \pm 7.5 | 9. m |
| 974.62 \pm 0.57 | 5500. \pm 1100. | 3700. \pm 420. | 2500. \pm 280. | 980. \pm 120. | 230. \pm 50. | 29. \pm 26. | --- | --- | 1.6m \pm 0.4m |
| 1010.45 \pm 0.44 | --- | --- | --- | --- | 300. \pm 50. | 280. \pm 40. | 170. \pm 20. | 61. \pm 7. | 35. m \pm 5 m ^g |
| 1024.53 \pm 0.95 | --- | --- | --- | --- | --- | --- | 31. \pm 16. | 20. \pm 5. | 97. m \pm 60 m |
| 1032.12 \pm 0.54 | --- | --- | 650. \pm 180. | 740. \pm 110. | 710. \pm 60. | 430. \pm 40. | 120. \pm 20. | 17. \pm 5. | 15. m ^h |

^f Precursor: 8 m \pm 2 m^g Precursor: 4 m^h Precursor: 3 m

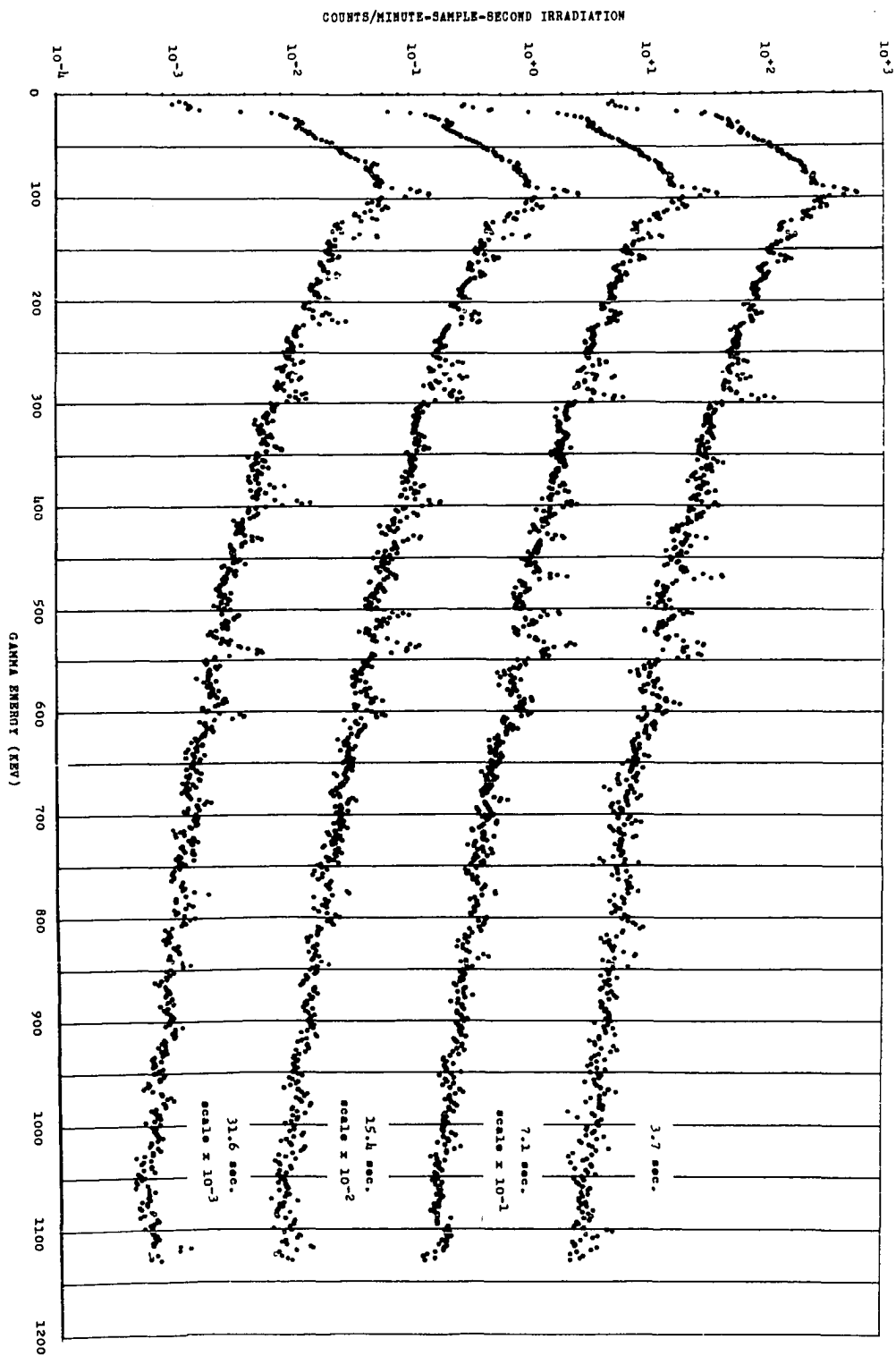
TABLE 4 (Continued)

| Gamma Energy (keV) | $\times 10^4$ dpm/sample - second irradiation | | | | | | | | Approximate Half-life |
|-----------------------|---|------------------|------------------|-----------------|----------------|-----|---------------|--------------|--------------------------|
| | 1 | 2 | 3 | 4 | 5 | 6 | 7 | 8 | |
| 1072.79 \pm 0.69 | --- | --- | --- | --- | --- | --- | 66. \pm 21. | 50. \pm 7. | 152. m \pm 90 m |
| 1079.08 \pm 1.15 | --- | --- | 510. \pm 200. | 170. \pm 100. | 120. \pm 40. | --- | --- | --- | 5. m \pm 3 m |
| 1095.22 \pm 0.73 | 4500. \pm 1200. | 1900. \pm 410. | 1200. \pm 220. | 520. \pm 110. | 140. \pm 40. | --- | --- | --- | 3. m \pm 1 m |
| 1118.08 \pm 0.69 | 7200. \pm 1300. | 3300. \pm 450. | 640. \pm 200. | --- | --- | --- | --- | --- | 47. s \pm 7 s |



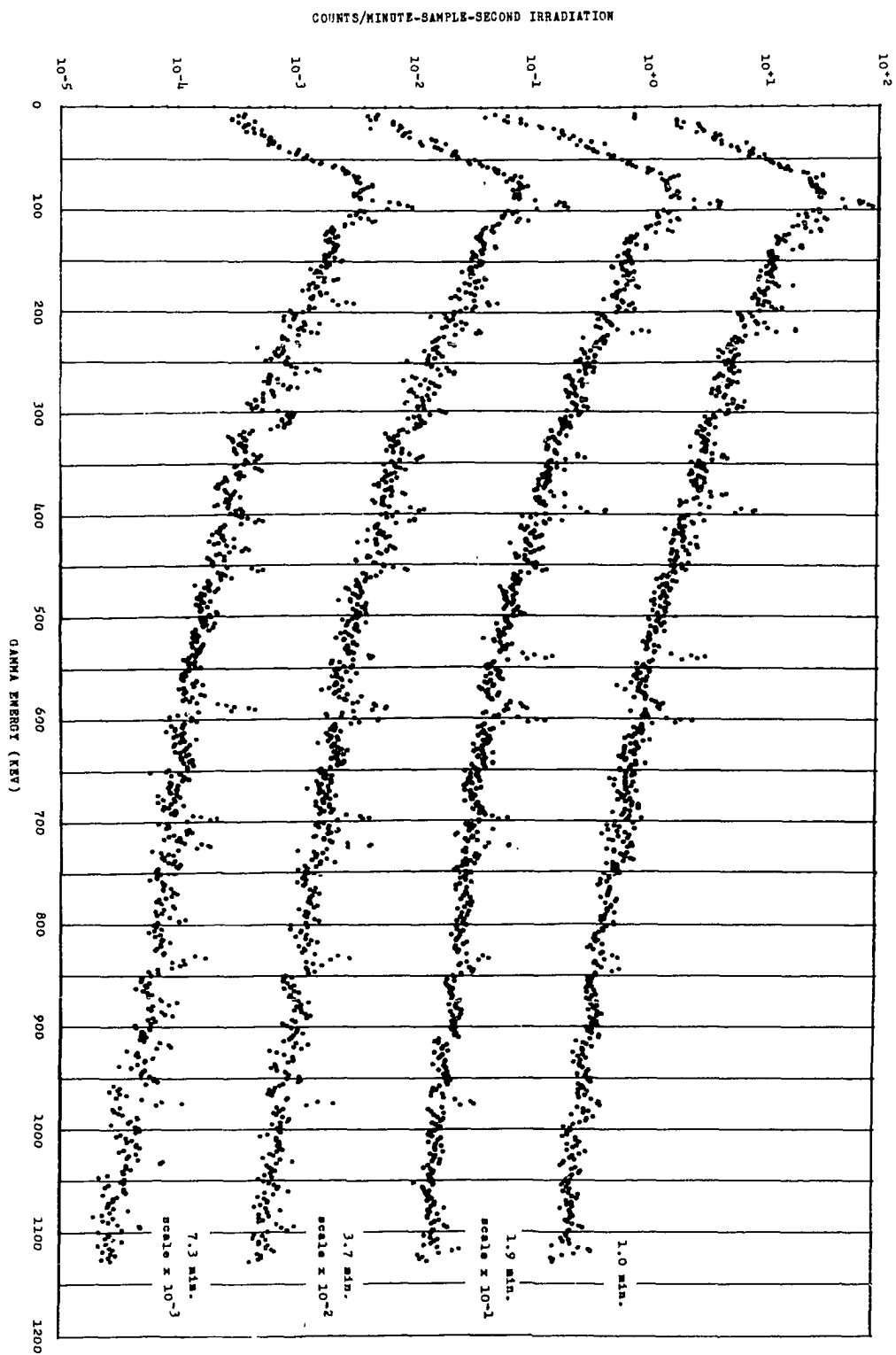
FISSION PRODUCT GAMMA RAY SPECTRA,
0.4-2.9 SECONDS AFTER FISSION

FIGURE 7



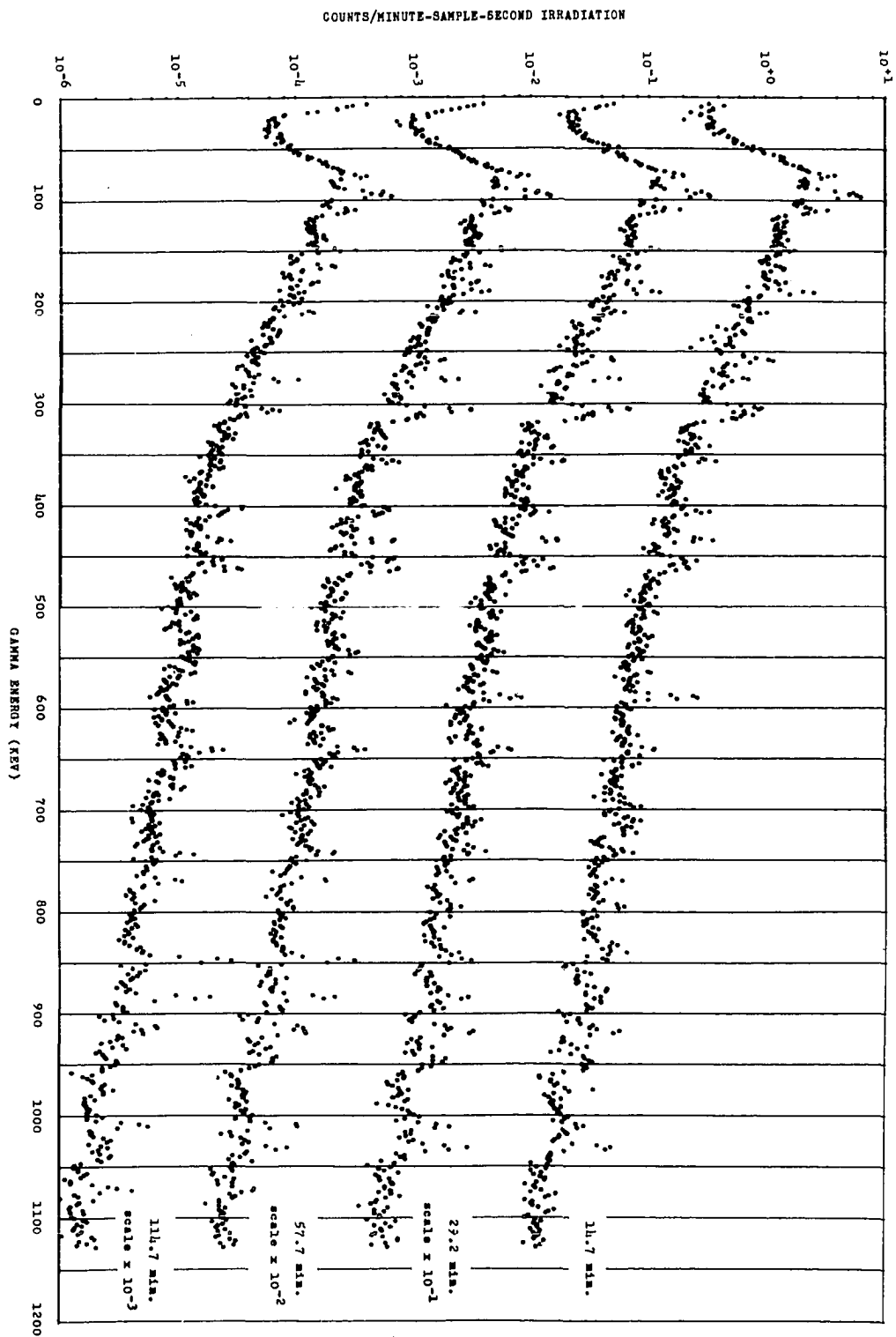
FISSION PRODUCT GAMMA RAY SPECTRA,
2.9-42.0 SECONDS AFTER FISSION

FIGURE 8



FISSION PRODUCT GAMMA RAY SPECTRA,
0.7-9.7 MINUTES AFTER FISSION

FIGURE 9



FISSION PRODUCT GAMMA RAY SPECTRA,
9.7-152.7 MINUTES AFTER FISSION

FIGURE 10

CHAPTER VI

DISCUSSION OF RESULTS

The half-lives listed in Tables 3 and 4 were determined by the usual procedure of plotting the values of the peak areas with their standard deviations versus time of observation on semi-logarithmic graph paper and determining the best straight line which can be drawn through the points. In most of the determinations listed the decay lines were drawn within the error limits of all points. In the cases where half-lives were not listed the decay curves appeared to contain more than one exponential component. The peaks appeared to decay very rapidly at first, but the decay rate would then start decreasing until in most instances it became a single exponential decay. There are two explanations for this type of behavior. One is that the decay represents the decay of a short half-life fission product having a longer-lived precursor. The short half-life fission product decays rapidly at first because of a higher yield than its precursor, but then eventually reaches equilibrium with the longer-lived precursor. Although this situation occurs many times in fission product decay chains having an even mass number, the scatter of the data is too great to warrant the conclusion that every decay curve of this type represents an even mass number decay. A more logical conclusion is that the decay curve represents

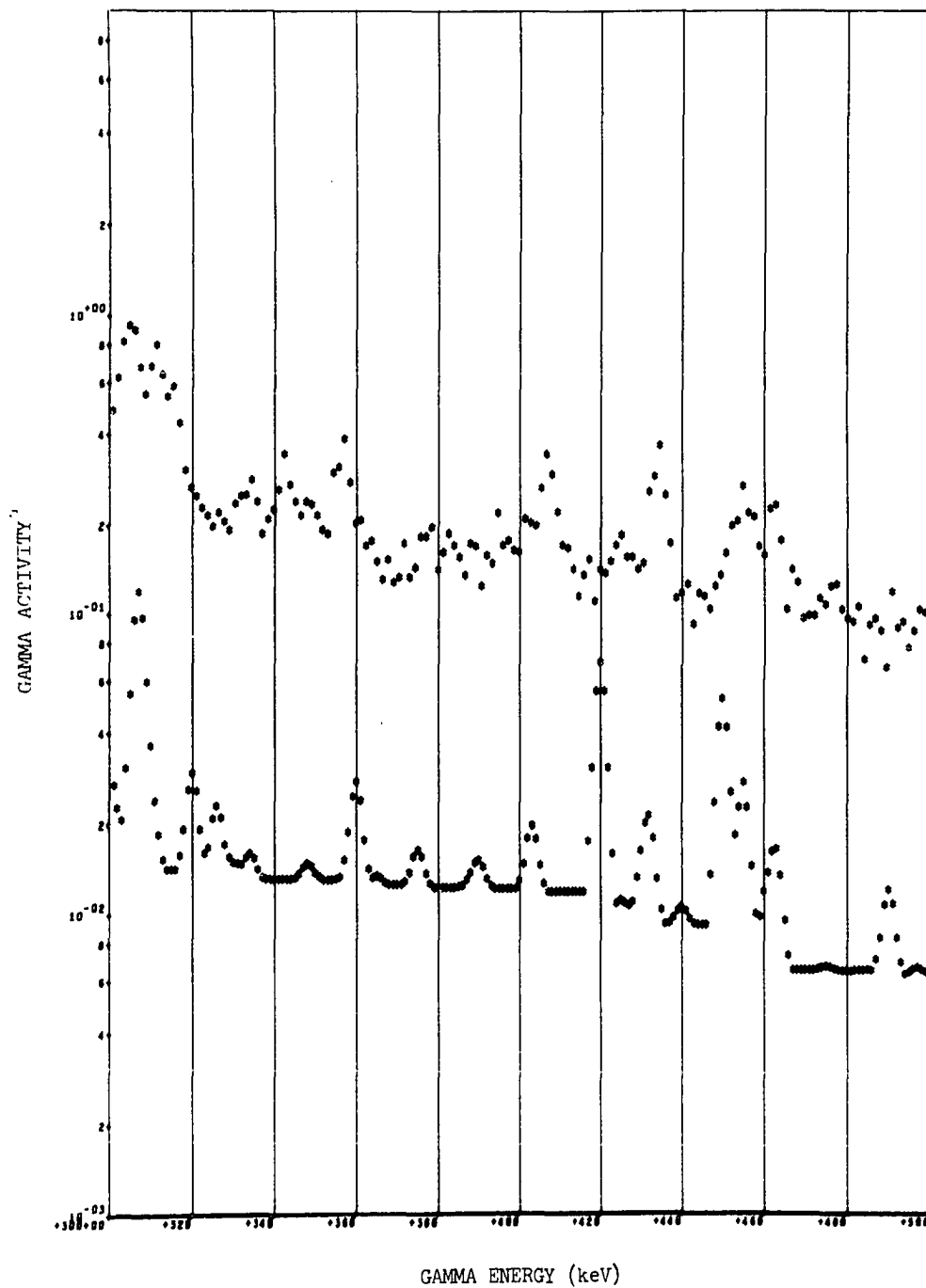
the decay of a peak containing two or more unresolved gamma rays. The density of gamma rays at low energies is high and the probability of having two or more gamma rays so close in energy that they are unresolvable is probably equal to the per cent occurrence of such decay curves, around 20 per cent.

Three X-rays from uranium are emitted with enough intensity to be detected but their energies are too close to be well resolved. The X-ray energies are 93.8 keV, 94.7 keV, and 98.44 keV.

Comparison of the data with the predicted spectra is good at the longer times after fission. This is as expected since more data are available and better known at the longer times than at the shorter times. Relative intensities and energies of the predicted spectra do not agree exactly with the experimental data but the general shapes are in good agreement. A comparison between the experimental data and the predicted spectrum at 14.7 minutes after fission appears in Fig. 11. The energy range of the spectra is from 300 keV to 500 keV.

With the aid of the predicted spectra some identification has been made. Prominent peaks in the experimental spectra were matched with the known peaks in the predicted spectra. Computed half-lives were also an aid in identification when they were matched with previously tabulated known half-lives. Twenty-eight gamma energies were assigned to fourteen fission products. These fission products along with their computed half-lives and gamma energies are listed in Table 5.

The largest errors in this study were in the determination of the half-lives which were directly related to the peak areas and



Comparison of Predicted Spectrum with Experimental
Spectrum at 14.7 Minutes After Fission

Figure 11

^a The figure is for qualitative comparison only. The intensity of the two spectra have not been normalized.

TABLE 5
IDENTIFIED FISSION PRODUCTS

| Fission Product | Half-life ^a | Gamma Energy | Fission Product | Half-life ^a | Gamma Energy |
|-------------------|------------------------|---------------------|---------------------------------|------------------------|--------------------|
| Kr ⁸⁷ | 72 m | 402.1 | Cs ¹⁴⁰ | 62 s | 601.5 |
| Rb ⁹⁰ | 4 m | 832.3 | Ba ¹⁴¹ | 19 m | 191.3 |
| Kr ⁹⁰ | 41 s | 120.6 | | | 277.3 |
| | | 539.4 | | | 305.7 |
| | | 1118.2 | | | 342.9 |
| Mo ¹⁰¹ | 12 m | 589.9 | | | 657.1 ^b |
| | | 1032.1 ^b | La ¹⁴² | 81 m | 641.3 |
| Xe ¹³⁷ | 3.2 m | 270.4 | | | 884.3 |
| | | 455.4 | Y ^{94^b} | 27 m | 743.1 |
| Cs ¹³⁸ | 34.5 m | 452.9 | | | 918.9 |
| | | 1010.4 | Te ^{133 m^b} | 52 m | 329.5 |
| Ba ¹³⁹ | 57 m | 166.0 | | | 462.4 |
| Xe ¹³⁹ | 45 s | 219.6 | | | 913.1 |
| | | 396.5 | Pr ^{148^b} | 4.5m | 301.8 |

^a Computed average half-lives

^b Possible assignment

their associated statistical uncertainty. These errors can be reduced by obtaining more counts per channel in the spectra, but since the count rate cannot be increased, one alternative is to make more observations. This can be done by using an automatic sample changer which runs continuously. In the same sampling period in which manual observations were made, an increase in the number of observations by at least a factor of ten could easily be obtained using such a device. Another alternative is to use a detector with a larger sensitive volume. This will increase the efficiency and thereby increase the number of pulses entering the analyzer. This increase will be more pronounced at the higher energies. For high energy observations lead absorbers can be used to filter out the low energy activity thus reducing the gross activity without appreciably attenuating the high energy portion of the spectrum.

Although the resolution was good, it can be significantly improved by placing the input stage of the preamplifier physically close to the detector thus reducing the length of the signal lead coming from the detector to the preamplifier. A reduction in lead length will reduce the capacitance into the preamplifier. Since the charge-sensitive preamplifier noise is proportional to capacitance, a shortening of the signal lead will decrease the component of resolution due to the electronics.

It is recommended that this study be extended to accumulate data in the high energy region of the spectrum, from 1 MeV to 6 MeV. Such observation should be done with as large a detector as possible operated in coincidence with the NaI annulus in the double-escape mode.

Other fissile isotopes, notably Pu^{239} and U^{233} , can be studied in the same manner and using the same equipment as described in Chapter IV. The spectra of Pu^{239} fission products would be slightly different because of the different yield-mass distribution.

LIST OF REFERENCES

1. Zigman, P., and Mackin, J. "Early Time Decay of Fission Product Mixtures. II Gamma Energy Release and Ionization Rates Following Thermal Neutron Fission of U^{235} ". USNRDL-TR 400, (1960).
2. Knabe, W. E., and Putman, G. E. "The Activity of the Fission Products of U^{235} ", APEX-448, (1958).
3. Zobel, W., and Love, T. A. "Spectrum of Fission-Product Gamma Rays Measured at Short Times After Uranium Sample Irradiations". Proceedings of the Shielding Symposium Held at the USNRDL, October, 1956, USNRDL-R and L-29, 1, (1957).
4. Peele, R., Zobel, W., and Love, T. A. "Measurement of the Spectrum of Short-Lived Fission Product Decay Gamma Rays Emitted from a Rotational Fuel Belt". Proceedings of the Shielding Symposium Held at the USNRDL, October, 1956, USNRDL-R and L-29, 1, (1957).
5. Maienschein, F. C. et al. "Gamma Rays Associated with Fission". Second U. N. International Conference on the Peaceful Uses of Atomic Energy, A/Conf. 15/P670 USA, (1958).
6. LaRiviere, P. D. "Early-Time Gamma Ray Properties of U^{235} Gross Fission Products". USNRDL-TM-89, (1958).
7. Perkins, J. F., and King, R. W. "Energy Release from the Decay of Fission Products", Nuclear Science and Engineering, 3:726, (1958).

8. Engle, L. B., and Fisher, P. C. "Energy and Time Dependence of Delayed Gammas from Fission", LASL Report LAMS 2642, (1962).
9. Petrov, Yu. I. "Gamma-Radiation of the Fission Fragments of U^{235} and Pu^{239} ", The Soviet Journal of Atomic Energy, 7, No. 2, (1961)
10. Miller, C. F. "Gamma Decay of Fission Products from the Slow Neutron Fission of U^{235} ". USNRDL-TR-187, (1957).
11. Miller, C. F. "Proposed Decay Schemes for Some Fission Product and Other Radionuclides". USNRDL-TR-160, (1957).
12. Bolles, R. C., and Ballou, N. E. "Calculated Activities and Abundances of U^{235} Fission Products". USNRDL 456, (1956).
13. Moteff, J. "Fission Product Decay Gamma Energy Spectrum", APEX-134, (1953).
14. Clark, F. H. "Decay of Fission Product Gammas", NDA-27-39, (1954).
15. McBean, I. J. "The Decay Energy of the Fission Products of U^{235} ", AERE M 494.
16. Armantrout, G. A., and Camp, D. C. "Lithium-Drifted Germanium Detectors for High Resolution Beta- and Gamma-Ray Spectroscopy", UCRL-12245, (1965).
17. John. W. Bull. Am. Phys. Soc., Ser. II, 11, No. 1, 30 (1966).
18. Nuclear Data Sheets, National Academy of Sciences-National Research Council, 5, Set 1, (1962).
19. Crocker, G. R., and Connors, M. A. "Gamma-Emission Data for the Calculation of Exposure Rates from Nuclear Debris", 1, USNRDL-TR-876, (1965).

20. Katcoff, S. "Fission Product Yields from Neutron-Induced Fission", *Nucleonics* 18, 11, 201, (1960).
21. England, T. R. "Time Dependent Fission Product Thermal and Resonance Absorption Cross Sections", WAPD-TM-333, (1962).
22. Pappas, A. C. : The Distribution of Nuclear Charge in Low-Energy Fissions, "Proceedings of the International Conference on the Peaceful Uses of Atomic Energy", 7, p. 19, United Nations, New York, (1956).
23. Trail, C. C., and Raboy, S. "Scintillation Spectrometer with an Anticoincidence Annulus of NaI (Tl)". *Rev. Sci. Instr.* 30 (1959) 425.
24. Hunter, H. F., and Ballou, N. E. "Simultaneous Slow-Neutron Fission of U^{235} Atoms, I. Individual and Total Rates of Decay of the Fission Products", USNRDL Report AD 65, (1949).
25. Faller, I. L., Chapman, T. S., and West, J. M. "Calculations on U^{235} Fission Product Decay Chains", ANL-4807, (1952).
26. Chasman, C., Jones, K. W., and Ristinen, R. A. "Fast Neutron Bombardment of a Lithium-Drifted Germanium Gamma-Ray Detector", BNL 9157, (1965).
27. Watson, J. E., Jr. "An Analysis of Calculated and Measured Fission Product Activities", BRL 1239, (1964).
28. Benedict, M., and Pigford, T. H. Nuclear Chemical Engineering, McGraw-Hill, New York, (1957).
29. Weinberg, A. M., and Wigner, E. P. The Physical Theory of Neutron Chain Reactors, The University of Chicago Press, Chicago, (1958).

30. Glasstone, S. Principles of Nuclear Reactor Engineering,
Van Nostrand, New York, (1955).

APPENDIX A

DERIVATION OF VARIATIONS OF THE BATEMAN EQUATIONS

Continuous Production

For simplicity consider a three-isotope chain:

Nuclide: $X \longrightarrow Y \longrightarrow Z$

Decay Constant: λ_1 λ_2

Z will be considered stable so its decay constant is zero. Consider a nuclear reaction in which U^{235} is undergoing fission at a constant rate, such that P_1 atoms of X are formed per unit time. The net rate of change of the number of X atoms N_1 is

$$\frac{dN_1}{dt} = P_1 - \lambda_1 N_1 \quad (A-1)$$

The net rate of change of the number of Y atoms N_2 is

$$\frac{dN_2}{dt} = \lambda_1 N_1 - \lambda_2 N_2 \quad (A-2)$$

The net rate of change of the number of Z atoms N_3 is

$$\frac{dN_3}{dt} = \lambda_2 N_2 \quad (A-3)$$

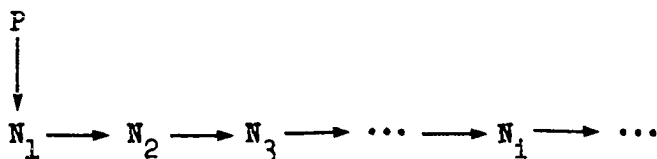
In the more general case in which the reactor is started at time zero with no fission products present and at that time starts generating X at a steady rate of P_1 atoms per unit time, the amounts of the individual members of the decay chain present at time t are obtained by integrating equations (A-1) to (A-3), with the boundary condition that each $N = 0$ at $t = 0$.

$$N_1 = \frac{P_1}{\lambda_1} (1 - e^{-\lambda_1 t}) \quad (\text{A-4})$$

$$N_2 = \lambda_1 P_1 \left[\frac{1 - e^{-\lambda_1 t}}{\lambda_1 (\lambda_2 - \lambda_1)} + \frac{1 - e^{-\lambda_2 t}}{\lambda_2 (\lambda_1 - \lambda_2)} \right] \quad (\text{A-5})$$

$$N_3 = P_1 t - (N_2 + N_1) \quad (\text{A-6})$$

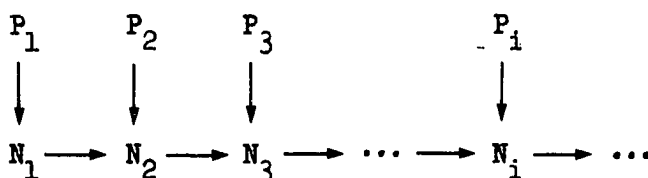
Consider a general description of a radioactive decay chain where the first member of the chain is produced at a constant rate P and other members are formed only by decay of their precursor:



If none of the members of the decay chain is present at time zero, the amount N_i of the i -th nuclide present at time t can be written by an extension of the derivation which led to equation (A-5):

$$N_i = \lambda_1 \lambda_2 \cdots \lambda_{i-1} P \sum_{j=1}^i \frac{1 - e^{-\lambda_j t}}{\lambda_j \prod_{k \neq j} (\lambda_k - \lambda_j)} \quad (A-7)$$

In the case of a fission product decay chain where each member of the chain is produced at a constant rate:



and if none of the members of the decay chain is present at time zero, the amount $N_{i,m}$ of the i -th nuclide present at time t due to the production of the m -th nuclide and decay of precursors is

$$N_{i,m} = \lambda_m \lambda_{m+1} \cdots \lambda_{i-1} P_m \sum_{j=1}^i \frac{1 - e^{-\lambda_j t}}{\lambda_j \prod_{k \neq j} (\lambda_k - \lambda_j)} \quad (A-8)$$

The total number of atoms N_i of the i -th nuclide present at time t is, therefore,

$$N_i = N_{i,1} + N_{i,2} + \cdots + N_{i,i} \quad (A-9)$$

Batch Decay

Suppose N_1^0 atoms of X are freshly purified at time zero. The

net rate of change of the number N_1 of X atoms is

$$\frac{dN_1}{dt} = -\lambda_1 N_1 \quad (\text{A-10})$$

The net rate of change of the number N_2 of Y atoms is

$$\frac{dN_2}{dt} = \lambda_1 N_1 - \lambda_2 N_2 \quad (\text{A-11})$$

The net rate of change of the number N_3 of Z atoms is

$$\frac{dN_3}{dt} = \lambda_2 N_2 \quad (\text{A-12})$$

The solution to equation (A-10), subject to $N_1 = N_1^0$ at $t = 0$, is

$$N_1 = N_1^0 e^{-\lambda_1 t} \quad (\text{A-13})$$

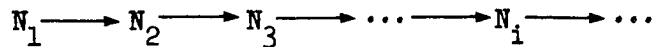
The solution to equation (A-11), subject to $N_2 = 0$ at $t = 0$, is

$$N_2 = \frac{\lambda_1 N_1^0}{\lambda_2 - \lambda_1} (e^{-\lambda_1 t} - e^{-\lambda_2 t}) \quad (\text{A-14})$$

Likewise, with $N_3 = 0$ at $t = 0$, equation (A-12) integrates to

$$N_3 = N_1^0 (1 - e^{-\lambda_1 t}) - N_2 \quad (\text{A-15})$$

In the general case of a radioactive decay chain



in which the parent material is present in an amount N_1^0 at time zero, if none of the other members of the decay chain is initially present, the amount N_i of any nuclide present at time t can be written by an extension of the derivation which led to equation (A-14):

$$N_i = \lambda_1 \lambda_2 \cdots \lambda_{i-1} N_1^0 \sum_{j=1}^i \frac{e^{-\lambda_j t}}{\prod_{k \neq j} (\lambda_k - \lambda_j)} \quad (A-16)$$

In the case of a fission product decay chain where each nuclide is initially present, equation (A-16) extends to

$$N_{i,m} = \lambda_m \lambda_{m+1} \cdots \lambda_{i-1} N_m^0 \sum_{j=1}^i \frac{e^{-\lambda_j t}}{\prod_{k \neq j} (\lambda_k - \lambda_j)} \quad (A-17)$$

and

$$N_i = N_{i,1} + N_{i,2} + \cdots N_{i,i} \quad (A-9)$$

Continuous Production and Shutdown

We shall assume the reactor started up at time zero with no fission products present, and all processes of removal of fission products other than by radioactive decay will be neglected. The reactor will be operating at a constant fission rate for a time T at which time the fission products are removed and allowed to undergo radioactive decay for an additional time t . The first member of the chain is produced at a constant rate P from time zero to T . The

amounts $N_1(T)$ and $N_2(T)$ of the first two nuclides of the decay chain present at time T when they are removed from the reactor - or when the reactor is shut down - are obtained from equations (A-4) and (A-5), respectively:

$$N_1(T) = \frac{P}{\lambda_1} (1 - e^{-\lambda_1 T}) \quad (A-18)$$

$$N_2(T) = \lambda_1 P \left[\frac{1 - e^{-\lambda_1 T}}{\lambda_1 (\lambda_2 - \lambda_1)} + \frac{1 - e^{-\lambda_2 T}}{\lambda_2 (\lambda_1 - \lambda_2)} \right] . \quad (A-19)$$

At the time t after shutdown ($t = 0$ at time T), the number $N_1(T, t)$ of atoms of the parent member of the chain is obtained by applying equation (A-13):

$$N_1(T, t) = N_1(T) e^{-\lambda_1 t} . \quad (A-20)$$

Combining with equation (A-18),

$$N_1(T, t) = \frac{\bar{P}}{\lambda_1} (1 - e^{-\lambda_1 T}) e^{-\lambda_1 t} . \quad (A-21)$$

Of the $N_2(T)$ atoms of the second nuclide present at $t = 0$, the number $N_{2,2}(T, t)$ which have not decayed by time t is

$$N_{2,2}(T, t) = N_2(T) e^{-\lambda_2 t} . \quad (A-22)$$

Combining with equation (A-19)

$$N_{2,2}(T,t) = \lambda_1 P \left[\frac{1 - e^{-\lambda_1 T}}{\lambda_1 (\lambda_2 - \lambda_1)} + \frac{1 - e^{-\lambda_2 T}}{\lambda_2 (\lambda_1 - \lambda_2)} \right] e^{-\lambda_2 t}. \quad (A-23)$$

The number of atoms of the second nuclide present at time t as a result of the decay of the $N_1(T)$ atoms of the first nuclide at time $t = 0$ is obtained by applying equation (A-14):

$$N_{2,1}(T,t) = \frac{\lambda_1 N_1(T)}{\lambda_2 - \lambda_1} (e^{-\lambda_1 t} - e^{-\lambda_2 t}). \quad (A-24)$$

Combining with equation (A-18)

$$N_{2,1}(T,t) = \frac{P}{\lambda_2 - \lambda_1} (1 - e^{-\lambda_1 T}) (e^{-\lambda_1 t} - e^{-\lambda_2 t}). \quad (A-25)$$

The total number $N_2(T,t)$ of atoms of the second nuclide present at time t is the sum of the number remaining from those present at time $t = 0$ and the number resulting from the decay of the first nuclide:

$$N_2(T,t) = N_{2,2}(T,t) + N_{2,1}(T,t). \quad (A-26)$$

Combining equations (A-23) and (A-24) to equation (A-26) and simplifying,

$$N_2(T,t) = \lambda_1 P \left[\frac{(1 - e^{-\lambda_1 T}) e^{-\lambda_1 t}}{\lambda_1 (\lambda_2 - \lambda_1)} + \frac{(1 - e^{-\lambda_2 T}) e^{-\lambda_2 t}}{\lambda_2 (\lambda_1 - \lambda_2)} \right] \quad (A-27)$$

The general equation is

$$N_i(T, t) = \lambda_1 \lambda_2 \cdots \lambda_i - 1^P \sum_{j=1}^i \frac{(1 - e^{-\lambda_j T}) e^{-\lambda_j t}}{\lambda_j \prod_{k \neq j} (\lambda_k - \lambda_j)} \quad (A-28)$$

For the case where each member of the decay chain is produced at a constant rate P_m , as in the continuous production case, while the reactor is operating

$$N_{i,m}(T, t) = \lambda_m \lambda_{m+1} \cdots \lambda_i - 1^P P_m \sum_{j=1}^i \frac{(1 - e^{-\lambda_j T}) e^{-\lambda_j t}}{\lambda_j \prod_{k \neq j} (\lambda_k - \lambda_j)} \quad (A-29)$$

and

$$N_i(T, t) = N_{i,1}(T, t) + N_{i,2}(T, t) + \cdots N_{i,i}(T, t) \quad (A-30)$$

In the cases where production is involved, the production rate for the i -th nuclide P_i is

$$P_i = N_f \sigma_f \varphi y_i \quad (A-31)$$

where N_f = the number of fissionable atoms present

σ_f = microscopic fission cross section for fissionable atoms

φ = neutron flux

y_i = fission yield for i -th nuclide

APPENDIX B

COMPUTER PROGRAM FOR THE PREDICTION OF FISSION-PRODUCT GAMMA-RAY SPECTRA

```

CFP65  DETERMINATION OF TIME DEPENDENT FISSION PRODUCT GAMMA RAY
C      SPECTRA VIA BATEMAN EQUATIONS OCTOBER 1965, BOGGS VERSION
C      JIS = NUMBER OF ISOTOPE IN DECAY CHAIN IC, KJ = NUMBER OF GAMMAS
C      PER PARTICULAR ISOTOPE. IEG, BR ARE THE ENERGIES AND BRANCHING
C      RATIOS, RESPECTIVELY. UY AND PUY ARE URANIUM AND PLUTONIUM FP
C      YIELDS. XMETA IS THE ISOMERIC TRANSITION BRANCHING RATIO.
C      STOP IC READ-BLANK CARD.1 ISOTOPE CHAIN-DUMMY 2ND. ISOMERIC NOT 1.
C      FOR INTEGRATION, MQA=MQ MQA IN COL. 78
C      DIMENSION ACT(5600),JIS(100),KJ(97,7),XLAM(97,7),XMETA(97,7),
1UY(97,7),PUY(97,7),IEG(97,7,18),BR(97,7,18),T(10),A(7,7),PSI(7,7),
2XI(7,7),MKJ(72,7),XMLAM(72,7),UYM(72,7),MIEG(72,7,13),BMR(72,7,13)
3,LIEG(20),QBR(20),X(5600)
DO 801 N=1,5600
X(N)=N
ACT(N)=0.0
801 CONTINUE
DO 4 IC=1,100
JIS(IC)=0
4 CONTINUE
DO 900 I=1,7
DO 900 N=1,97
KJ(N,I)=0
XLAM(N,I)=0.0
XMETA(N,I)=0.0
UY(N,I)=0.0
PUY(N,I)=0.0
900 CONTINUE
DO 901 M=1,18
DO 901 L=1,7
DO 901 N=1,97
IEG(N,L,M)=0
BR(N,L,M)=0.0
901 CONTINUE

```

```

DO 902 L=1,7
DO 902 N=1,72
MKJ(N,L)=0
XMLAM(N,L)=0.0
UYM(N,L)=0.0
902 CONTINUE
DO 903 M=1,13
DO 903 L=1,7
DO 903 N=1,72
MIEG(N,L,M)=0
BMR(N,L,M)=0.0
903 CONTINUE
PRINT 8888
8888 FORMAT (1H1,18HLIST OF INPUT DATA)
2 READ (10,1000) (IC,JIS(IC))
PRINT 7777,IC,JIS(IC)
7777 FORMAT (1X,3HIC=,14,4X,4HJIS=,14,10H*****
IF(IC)1,99,1
1 J=JIS(IC)
IF(J)79,2,79
79 READ (10,1001) (KJ(IC,L),XLAM(IC,L),XMETA(IC,L),L=1,J)
READ(10,1002)(UY(IC,KL),KL=1,J)
PRINT 10011,(KJ(IC,L),XLAM(IC,L),XMETA(IC,L),L=1,J)
PRINT 10021,(UY(IC,KL),KL=1,J)
DO3NJ=1,J
K=KJ(IC,NJ)
PRINT 1111,IC,NJ,K
IF(K)78,3,78
78 READ(10,1003)(IEG(IC,NJ,KR),BR(IC,NJ,KR),KR=1,K)
PRINT 10030
PRINT 10031,(IEG(IC,NJ,KR),BR(IC,NJ,KR),KR=1,K)
10031 FORMAT (1X,10(1X,I4,1X,F5.3,1X))
C ISOMERIC READ-IN IF ANY
IF(XMETA(IC,NJ))3,3,17
17 READ(10,1007)MKJ(IC,NJ),XMLAM(IC,NJ),UYM(IC,NJ)
K=MKJ(IC,NJ)
PRINT 10071, MKJ(IC,NJ),XMLAM(IC,NJ),UYM(IC,NJ)
PRINT 10070
READ(10,1003)(MIEG(IC,NJ,KR),BMR(IC,NJ,KR),KR=1,K)
PRINT 10031,(MIEG(IC,NJ,KR),BMR(IC,NJ,KR),KR=1,K)
3 CONTINUE
10070 FORMAT (2X,8HMIEG,BMR)
10071 FORMAT (1X,13HMKJ,XLAM,UYM,2X,14,1X,2(E8.3,1X))
10030 FORMAT (1X,6HIEG,BR)
1111 FORMAT (1X,3HIC=,14,5X,3H NJ=,14,5X,2HK=,14)
10011 FORMAT (1X,13HKJ,XLAM,XMETA,4X,6(12,1X,E8.3,1X,F3.2,2X))
10021 FORMAT (1X,2HUY,4X,10(E8.3,2X))
GOTO2
99 READ (10,1004) (MQ,(T(MT),MT=1,MQ))
READ (10,1009) ZA,WA,ZB,WB,ZC,ZD,WD,QQ,QK,PER,MQA
DO 100 MT=1,MQ

```

```

      PRINT 995
995  FORMAT (1H1, 5X, 12HCHAIN NUMBER, 10X, 7HISOTOPE, 10X, 16HISOTOPE ACTIVI
      1TY, 10X, 12HGAMMA ENERGY, 10X, 14HGAMMA ACTIVITY//)
      IF (MQA-MT) 181, 182, 182
181  DO 18 L=1, 5600
      ACT(L)=0.0
      18 CONTINUE
182  DO 500 IC=1, 97
      R=0.0
      IF (JIS(IC)) 81, 500, 81
      81 TC=T(MT)
      JO=JIS(IC)
      DO 6 J=1, JO
      IF (XLAM(IC, J)*TC-87.0) 7, 8, 8
      7 A(J, J)=UY(IC, J)*1.0/EXP(XLAM(IC, J)*TC)
      GOTO 6
      8 A(J, J)=0.0
      6 CONTINUE
      DO 300 I=2, JO
      IF (XLAM(IC, I)) 9, 300, 9
      9 IF (KJ(IC, I)) 11, 300, 11
11  N=I-1
      DO 14 K=1, N
      PS=UY(IC, K)
      DO 5 M=K, N
      PS=PS*XLAM(IC, M)
      5 CONTINUE
      PSI(I, K)=PS
14  CONTINUE
      DO 15 M=1, N
      ZIP=0.0
      DO 82 K=M, I
      IF (XLAM(IC, K)*TC-87.0) 25, 26, 26
      25 XIP=1.0/EXP(XLAM(IC, K)*TC)
      GOTO 27
      26 XIP=0.0
      27 L=M
      12 IF (L-K) 87, 88, 87
      88 IF (L-I) 89, 13, 89
      89 L=L+1
      87 XIP=XIP/(XLAM(IC, L)*XLAM(IC, K))
      IF (L-I) 10, 13, 10
      10 L=L+1
      GOTO 12
      13 ZIP=XIP+ZIP
      82 CONTINUE
      XI(I, M)=ZIP
      A(I, M)=PSI(I, M)*XI(I, M)
15  CONTINUE
      AP=0.0
      DO 16 M=1, I

```



```

      AP=AP+A(I,M)
16  CONTINUE
      PURP=XLAM(IC,I)*AP
      PRINT 996,IC,I,PURP
996  FORMAT (1H ,11X,I3,16X,I2,16X,E9.4)
      MK=KJ(IC,I)
      DO400MO=1,MK
      IF(R)33,43,33
33  LIEG(MO)=IEG(IC,I,MO)
      IEG(IC,I,MO)=MIEG(IC,I,MO)
      QBR(MO)=BR(IC,I,MO)
      BR(IC,I,MO)=BMR(IC,I,MO)
43  IJK=IEG(IC,I,MO)
      TIJK=IJK
      IF (IJK-2800) 101,101,102
101  XINT=ZA*1.0/EXP(TIJK*WA)+ZB*1.0/EXP(TIJK*WB)
      SIG=(SQRT(QK+(QQ*TIJK)))*0.425
      GO TO 103
102  XINT=ZC-ZD*EXP(WD*TIJK)
      SIG=(SQRT(QK+(QQ*(TIJK-1022.)))*0.425
103  IF (XMETA(IC,I)) 41,44,41
      44  PACT=BR(IC,I,MO)*XINT*PURP
      GO TO 399
      41  PACT=XMETA(IC,I)*BR(IC,I,MO)*XINT*PURP
399  IG=SIG*2.0+2.0
      PRINT 997,IEG(IC,I,MO),PACT
997  FORMAT (1H ,73X,15,17X,E9.4)
      ACT(IJK)=(PACT/2.506)*(1.0/SIG) + ACT(IJK)
      DO 200 MOPR=2,IG
      Y=0.0
      MAP=MOPR-1
      NPEP= IJK-MAP
      XMAP=MAP
104  ACT(NPEP)=(PACT/2.506)*(1.0/SIG)*1.0/EXP((0.5*XMAP*XMAP)/(SIG*SIG)
      1) + ACT(NPEP)
      IF (MOPR-1) 200,200,93
93  IF (Y) 200,94,200
94  NPEP= IJK+MAP
      Y=1.0
      GO TO 104
200  CONTINUE
      IIJK=IJK-3
      DO 401 MP=1,IIJK
      ACT(MP)=PER*PACT+ACT(MP)
401  CONTINUE
400  CONTINUE
      IF(XMETA(IC,I))300,300,49
49  IF (R) 299,46,299
46  IF (XMLAM(IC,I)*TC-87.0) 47,48,48
48  A(I,I)=0.0

```

```

      AP=AP+A(I,M)
16  CONTINUE
      PURP=XLAM(IC,I)*AP
      PRINT 996,IC,I,PURP
996  FORMAT (1H ,11X,I3,16X,I2,16X,E9.4)
      MK=KJ(IC,I)
      DO400MO=1,MK
      IF(R)33,43,33
33  LIEG(MO)=IEG(IC,I,MO)
      IEG(IC,I,MO)=MIEG(IC,I,MO)
      QBR(MO)=BR(IC,I,MO)
      BR(IC,I,MO)=BMR(IC,I,MO)
43  IJK=IEG(IC,I,MO)
      TIJK=IJK
      IF (IJK-2800) 101,101,102
101  XINT=ZA*1.0/EXP(TIJK*WA)+ZB*1.0/EXP(TIJK*WB)
      SIG=(SQRT(QK+(QQ*TIJK)))*0.425
      GO TO 103
102  XINT=ZC-ZD*EXP(WD*TIJK)
      SIG=(SQRT(QK+(QQ*(TIJK-1022.))))*0.425
103  IF (XMETA(IC,I)) 41,44,41
      44  PACT=BR(IC,I,MO)*XINT*PURP
      GO TO 399
      41  PACT=XMETA(IC,I)*BR(IC,I,MO)*XINT*PURP
399  IG=SIG*2.0+2.0
      PRINT 997,IEG(IC,I,MO),PACT
997  FORMAT (1H ,73X,15,17X,E9.4)
      ACT(IJK)=(PACT/2.506)*(1.0/SIG) + ACT(IJK)
      DO 200 MOPR=2,IG
      Y=0.0
      MAP=MOPR-1
      NPEP= IJK-MAP
      XMAP=MAP
104  ACT(NPEP)=(PACT/2.506)*(1.0/SIG)*1.0/EXP((0.5*XMAP*XMAP)/(SIG*SIG)
      1) + ACT(NPEP)
      IF (MOPR-1) 200,200,93
93  IF (Y) 200,94,200
94  NPEP= IJK+MAP
      Y=1.0
      GO TO 104
200  CONTINUE
      IIJK=IJK-3
      DO 401 MP=1,IIJK
      ACT(MP)=PER*PACT+ACT(MP)
401  CONTINUE
400  CONTINUE
      IF(XMETA(IC,I))300,300,49
49  IF (R) 299,46,299
46  IF (XMLAM(IC,I)*TC-87.0) 47,48,48
48  A(I,I)=0.0

```

```

      GO TO 42
42  A(I,I)=UYM(IC,I)*1.0/EXP(XMLAM(IC,I)*TC)
47  DC=XLAM(IC,I)
      XLAM(IC,I)=XMLAM(IC,I)
      NKJ=KJ(IC,I)
      KJ(IC,I)=MKJ(IC,I)
      G=UY(IC,I)
      UY(IC,I)=UYM(IC,I)
      XMETA(IC,I)=1.0-XMETA(IC,I)
      R=1.0
      GOTOLL
299 R=0.0
      XLAM(IC,I)=DC
      KJ(IC,I)=NKJ
      UY(IC,I)=G
      DO 301 MO=1,MK
      IEG(IC,I,MO)=LIEG(MO)
      BR(IC,I,MO)=QBR(MO)
301 CONTINUE
300 CONTINUE
      PURP=XLAM(IC, )*A(1,1)
      I=1
      PRINT 996, IC, I, PURP
      MK=KJ(IC,I)
      IF (XMLAM(IC,I))) 500,500,303
303 IF (MK) 500,500,302
302 DO502MO=1,MK
      IJK=IEG(IC,I,MO)
      TIJK=IJK
      IF (IJK-2800) 201,201,202
201 XINT=ZA*1.0/EXP(TIJK*WA)+ZB*1.0/EXP(TIJK*WB)
      SIG=(SQRT(QK+(QQ*TIJK)))*0.425
      GO TO 244
202 XINT=ZC-ZD*EXP(WD*TIJK)
      SIG=(SQRT(QK+(QQ*(TIJK-1022.)))*0.425
244 PACT=BR(IC,I,MO)*XINT*PURP
      PRINT 997, IEG(IC,I,MO), PACT
      IG=SIG*2.0+2.0
      ACT(IJK)=(PACT/2.506)*(1.0/SIG) + ACT(IJK)
499 DO 700 MOPR=2, IG
      Y=0.0
      MAP=MOPR-1
      NPEP= IJK-MAP
      XMAP=MAP
204 ACT(NPEP)=(PACT/2.506)*(1.0/SIG)*1.0/EXP((0.5*XMAP*XMAP)/(SIG*SIG)
1) + ACT(NPEP)
      IF (MOPR-1) 700,700,293
293 IF (Y) 700,294,700
294 NPEP= IJK+MAP
      Y=1.0
      GO TO 204

```

```

700 CONTINUE
    IIJK=IJK-3
    DO 501 MP=1, IIJK
        ACT(MP)=PER*PACT+ACT(MP)
501 CONTINUE
502 CONTINUE
500 CONTINUE
    IF (MQA-MT) 802,802,100
802 TACT =0.0
    DO 800 IJK=1, 5600
        TACT=ACT(IJK)+TACT
800 CONTINUE
    WRITE(9,1005)TC
    DO600L=10, 5600, 10
    ML=L-9
    WRITE(9,1006)(ACT(IJK), IJK=ML,L), L
600 CONTINUE
    WRITE (9,1010) TACT
    YUBND=ACT(1)*10.0
    YLEND=ACT(2500)/50.0
706 DO 701 N=1, 5600
    IF (ACT(N)) 702,702,703
702 ACT(N)=YLEND
703 ACT(N)=ALOG10(ACT(N))
701 CONTINUE
    YUBND=ALOG10(YUBND)
    YLEND=ALOG10(YLEND)
    DO 105 IJK=1, 5500, 1100
    NIJK=IJK+1099
    MIJK=IJK-1
    CALL DGA (120,1000,0,890,MIJK,NIJK,YUBND,YLEND)
    CALL DLNLG (55)
    CALL DLNLG (11)
    CALL SBLIN (11,0)
    CALL SLLOG
    CALL PLOT (1100,X(IJK),1,ACT(IJK),1,42,1)
    CALLLLINCNT (60)
    WRITE(12,1008) IJK,NIJK,TC
    CALLADV(1)
105 CONTINUE
100 CONTINUE
1000 FORMAT(2I4)
1001 FORMAT (6(I2,E8.3,F3.2))
1002 FORMAT(10E8.3)
1003 FORMAT(10(I4,F4.3))
1004 FORMAT(I3,9F8.3)
1005 FORMAT(1H1,10X,22HTIME OF OBSERVATION = ,F8.3,15H MIN.AFTER FISS/)
1006 FORMAT(1H ,5X,10(E9.4,2X),I4)
1007 FORMAT(I4,2E8.3)
1008 FORMAT(10X,15HENERGY RANGE = ,I4,4H TO ,I4,15H KEV    TIME = ,
    1F8.3,4H MIN)

```

```
1009 FORMAT (7E9.4,F5.4,F4.3,F4.3,I2)
1010 FORMAT (1H0,10X,17HTOTAL ACTIVITY = ,E14.8)
      STOP
      END
```

